INFORMATION TO USERS

This manuscript has been reproduced from the microfilm master. UMI films the text directly from the original or copy submitted. Thus, some thesis and dissertation copies are in typewriter face, while others may be from any type of computer printer.

The quality of this reproduction is dependent upon the quality of the copy submitted. Broken or indistinct print, colored or poor quality illustrations and photographs, print bleedthrough, substandard margins, and improper alignment can adversely affect reproduction.

In the unlikely event that the author did not send UMI a complete manuscript and there are missing pages, these will be noted. Also, if unauthorized copyright material had to be removed, a note will indicate the deletion.

Oversize materials (e.g., maps, drawings, charts) are reproduced by sectioning the original, beginning at the upper left-hand corner and continuing from left to right in equal sections with small overlaps.

Photographs included in the original manuscript have been reproduced xerographically in this copy. Higher quality 6" x 9" black and white photographic prints are available for any photographs or illustrations appearing in this copy for an additional charge. Contact UMI directly to order.

ProQuest Information and Learning
300 North Zeeb Road, Ann Arbor, MI 48106-1346 USA
800-521-0600

SULFIDE STRESS CRACKING OF DISSIMILAR METAL WELDS

BY

Gasem Mohammed Fallatah

A Thesis Presented to the

DEANSHIP OF GRADUATE STUDIES

KING FAHD UNIVERSITY OF PETROLEUM & MINERALS

DHAHRAN, SAUDI ARABIA

In Partial Fulfillment of the
Requirements for the Degree of

MASTER OF SCIENCE

In

MECHANICAL ENGINEERING

صفر ١٤٢٢

(May 2001)

KING FAHD UNIVERSITY OF PETROLEUM & MINERALS

Dhahran 31261, Saudi Arabia

DEANSHIP OF GRADUATE STUDIES

This thesis, written by

GASEM MOHAMMED FALLATAH

Under the direction of his Thesis Advisor and approved by his Thesis Committee, has been presented to and accepted by the Dean of the College of Graduate Studies, in partial fulfillment of the requirement of the degree of

MASTER OF SCIENCE IN MECHANICAL ENGINEERING

Thesis Committee

Anwar Khalil Sheikh

Dr. Anwar K. Sheikh (Chairman)

Dr. Zafarullah Khan (Co-Chairman)

Dr. Zaki Ahmad (Member)

Dr. Yaagoub Al-Nassar (Member)

John Kwadwo Boah

Dr. John K. Boah (Member)

13/9/1422

Dr. Abdulghani A. Al-Farayedhi
Department Chairman

13/9/1422

Dean, College of Graduate Studies
Prof. Osama A. Jannadi

To my Father, Mother, and my Wife with love.

To all those who shared their care and concern.

ACKNOWLEDGMENT

Thanks to Allah who gave me the wisdom and strength needed to accomplish this work. Acknowledgment is due to Saudi Aramco for support of this study. It is also due to the Mechanical Engineering Department in King Fahd University of Petroleum & Minerals for support I got throughout my program.

The patience, guidance and generous support offered by my thesis advisor Prof. Anwar Khalil Sheikh and the co-advisor Dr. Zafrullah Khan in conducting this work is deeply appreciated.

I am also grateful to the other committee members, Dr. John Boah, Dr. Zaki Ahmed, and Dr. Yaagoub N. Al- Nassar.

And of course my family deserves the greatest appreciation for their support, patience, and encouragement throughout my program.

TABLE OF CONTENTS

LIST OF TABLES

LIST OF FIGURES

العنـــــوان : التصدع الكبريتيدي للمعادن غير المتشابهة الملحومة
الاســـــــم : قاسم محمد عبد الله فلاته
التخصـــص : الهندســـة الميكانيكيـة
تاريخ الشهـادة : صفر ١٤٢٢ الموافق مايو ٢٠٠١

تنامى في السنوات الأخيرة الاهتمام بمدى صلاحية المعادن غير المتشابهة الملحومة في البيئات الحمضية . والسبب الرئيسي لهذا الاهتمام هو أن هذه المعـــادن غـــير المتشـــابهة الملحومة تكون جسيمات صغيرة جداً وذات صلابة عالية جداً مما يـــــؤدي إلى إمكانيـــة حدوث التصدع الكبريتيدي فيها .

الهدف من هذه الدراسة هو تقييم مدى إمكانية حدوث التصـــــدع الكـــبريتيدي للمعادن غير المتشابهة الملحومة والمعدة بطريقة التسخين المسبق (في درجات حرارة مختلفة) ومعرضة لبيئة حمضية . ولقد تم استخدام طريقة الاختبار المعتمدة من الجمعيـــــة الأهليـــة لمهندسي التآكل تي أم - ٠١ - ٧٧ (الطريقة أ) لتقييـــــم إمكانيـــة حـــدوث التصـــدع الكبريتيدي في هذه العينات . لقد استخدمت الاختبارات المعد غرافية والوصف التصويري بمجهر المسح الإلكتروني لتحليل وتحديد ماهية التصدع الحادث . كما تم استخدام جـــهاز الـــ اي دي اس وقياس الصلابة المجهرية للتأكد من صحة المعلومات والنتائج.

أظهرت نتائج الاختبارات تحسن ملموس في الوقت اللازم لإحداث التصدع عنـــد استخدام طريقة التسخين المسبق في اللحام . إلا أنه وبالاستناد إلى متطلبات المواصفـــــات العالمية فإن العينات التي أعدت وفق الشروط المنصوص عليها في هذه الدراسة تعتبر قابلـــة للتصدع الكبريتيدي .

درجة الماجستير
جامعة الملك فهد للبترول والمعـادن
الظهران ، المملكة العربية السعودية
صفر ١٤٢٢
(مايو ٢٠٠١)

ABSTRACT

Title: **SULFIDE STRESS CRACKING OF DISSIMILAR METAL WELDS**

By: **GASEM MOHAMMED FALLATAH**

Major Field: **Mechanical Engineering**

Date: **May 2001**

Serious concerns have been raised in recent years in the Oil & Gas Industry about the reliability of Dissimilar Metal Welds (DMWs) in sour service. The primary reason for these concerns is because DMWs joint exhibit small localized hard zones that are susceptible to Sulfide Stress Cracking (SSC). In the open literature some methods such as preheating have been suggested to overcome the problem of these hard zone formation.

The objective of this study is to assess the susceptibility to Sulfide Stress Cracking (SSC) of DMWs specimens fabricated with different preheat temperatures and electrodes exposed to sour service environment. The National Association of Corrosion Engineers (NACE) Standard Tensile Test TM 01-77 Method A was used to determine DMWs susceptibility to SSC. Metallographic examination and Scanning Electron Microscope (SEM) characterization were used to assess the susceptibility and the failure modes. Energy Dispersive X-Ray Spectrometry (EDS) and Microhardness surveys were also performed to confirmer the finding of previous analysis.

Test results show considerable improvement in the Time-To-Failure as a result of the preheating methods used. However, and based on the standards requirements, Dissimilar Metal Welds fabricated in accordance to the welding conditions, and procedure used in this study are susceptible to sulfide stress cracking, and none of the welding condition used has based the SSC test.

MASTER OF SCIENCE

KING FAHD UNIVERSITY OF PETROLEUM & MINERALS
Dhahran, Saudi Arabia
May 2001

NOMENCLATURE

A	Actual Cross-Sectional Area
A_0	The Initial Cross-Sectional Area
A_f	The Final Cross-Sectional Area
ASTM	American Society for Testing Materials
°C	Degree Celsius
DMW	Dissimilar Metal Weld
EDS	Energy Dispersive X-ray Spectrometry
EFC	European Federation of Corrosion
% El	Percent Elongation
e^-	Electron
°F	Degree Fahrenheit
H_{ad}	Adsorbed Hydrogen
H_{ab}	Absorbed Hydrogen
H^+	Hydrogen ion
HS^-	Hydrogen Sulfide ion
HAZ	Heat-Affected Zone
HRC	Hardness Rockwell C
Ksi	Kilo Pound per Square Inch
L	Length
l_0	The Initial Specimen Length
l_f	The Final Specimen Length
NACE	National Association for Corrosion Engineers
P	Load
pH	Hydrogen Ions Concentration
%RA	Percent Reduction in Area
SSC	Sulfide Stress Cracking

T	Thickness
TTF	Time-To-Failure
VHN	Vickers Hardness Number
W	Width
Wt%	Weight Percent
Y.S.	Yield Strength
μ	Micron, 10^{-6}

CHAPTER 1

INTRODUCTION & BACKGROUND

1.1 Introduction

Dissimilar metal welds (DMWs) such as joining of ferritic steels, that is carbon and low alloy steels, to either austenitic stainless steels or nickel-base alloys are frequently required in the petroleum and petrochemical industries. Depending on the application, these welds are usually welded using either the austenitic stainless steel filler metals (electrods) or the nickel-base filler metals.

Serious concerns have been raised in recent years about the reliability of dissimilar metal welds. The primary reason for these concerns is because DMW joints exhibit small-localized zones along the fusion line that have very high hardness values exceeding VHN (400) [1]. These zones might be susceptible to Sulfide Stress Cracking (SSC) in wet sour service as per NACE MR 01-75 standard [2] because of their high hardness.

Although the problems inherent with DMW joints operating at elevated temperatures have long been recognized and understood, limited attention have been given to the sulfide stress corrosion cracking of these dissimilar joints. Similarly the literature on

strategies to overcome the cracking problem associated with DMW joints in H_2S environment is limited. DMWs have very complex metallurgical structures with significant variation in strain, and material properties. In the presence of H_2S, and depending on the environmental, micro-structural, and metallurgical conditions, DMWs can undergo SSC.

1.2 Significance of the Work

In Saudi Aramco, dissimilar metal welds were used to join carbon steel to 316 stainless steel in the Khuff gas gathering system and in the Uthmaniyah and Shedgum gas plants, which handle other sour gases in addition to the Khuff gas. These joint were used for seal welds, for fillet welds and, less commonly, for butt welds.

In 1984 a leak occurred when one of the dissimilar welds cracked due to sulfide stress cracking. Failure analysis indicated extermely high hardnesses around the weld fusion line. A survey of the facilities detected a number of other cracked welds. All such welds were removed immediately.

In 1988, failures of two DMWs at Uthmaniyah Trunkline # 1 and 2 due to SSC were reported. The two welds were not removed during the replacement program conducted in 1984.

In 1997, expansion in some sour gas handling facilities brought the issue of DMWs suitability again. Several ways were proposed to overcome the problem of SSC in DMWs. A study was needed to evaluate the proposed solutions.

1.3 Sulfide Stress Cracking Background

Sulfide stress cracking is defined as brittle failure at stresses well below the yield strength caused by cracking under the combined action of tensile stress and corrosion in the presence of water and hydrogen sulfide [3]. It is the result of very complex interactions of different parameters [2] including:

1) Hydrogen ion concentration (pH), H_2S concentration, and the total pressure of the environment.
2) Microstructure, chemical composition, strength, and the heat treatment of the material.
3) Total tensile stress applied and the level of residual stress (which could be introduced from welding).
4) Temperature, and time.

1.3.1 Sulfide Stress Cracking Mechanism

The mechanism of SSC in wet H_2S is illustrated by the following equations [2]:

1) H_2S dissociates in aqueous solution:

   $H_2S \rightarrow H^+ + HS^-$.

2) The anodic reaction during corrosion is:

   $Fe + HS^- \rightarrow FeS + H^+ + 2e^-$, and

3) The cathodic reaction is:

   $2H^+ + 2e^- \rightarrow 2H_{ad} \rightarrow H_2$, part of the adsorbed hydrogen, H_{ad}, is absorbed into the steel, H_{ab}.

The hydrogen is generated on the surface of the steel because of a corrosion reaction. Iron reacts with H_2S to form sulfide and hydrogen [5]. The hydrogen is generated in atomic form on the steel (or sulfide) surface, where it can either combine to form molecular hydrogen and leave the surface as bubbles or diffuse into the steel. This later process may result in hydrogen embrittlement or SSC. Hydrogen sulfide prevents hydrogen recombination and thus promotes entry of atomic hydrogen into the steel. It is important to note that water must be present for this mechanism to occur, because the ionization of the hydrogen sulfide is required [5].

After diffusing inside the material, the H-atoms locate themselves at the defects, inclusions, precipitates, and dislocation sites. This mechanism causes "perpendicular cracking" normal to the applied stress directions, which is known as hydrogen sulfide stress corrosion cracking. Figures 1.1, and 1.2 are schematic illustration for the SSC mechanism.

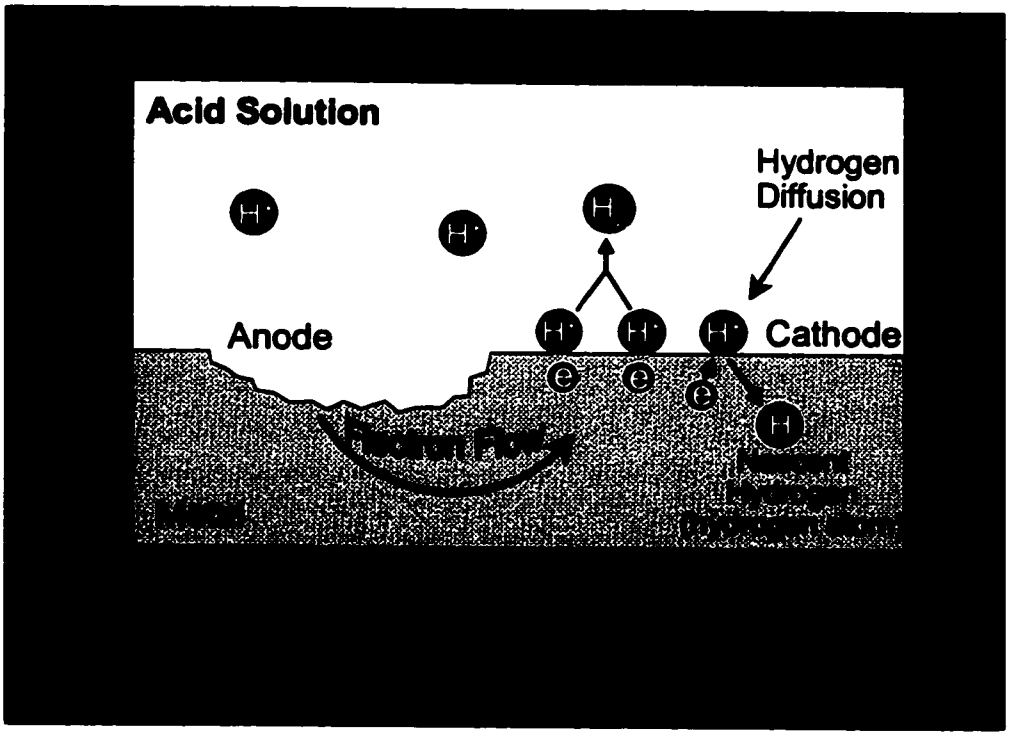

Figure 1.1. Hydrogen Diffusion.

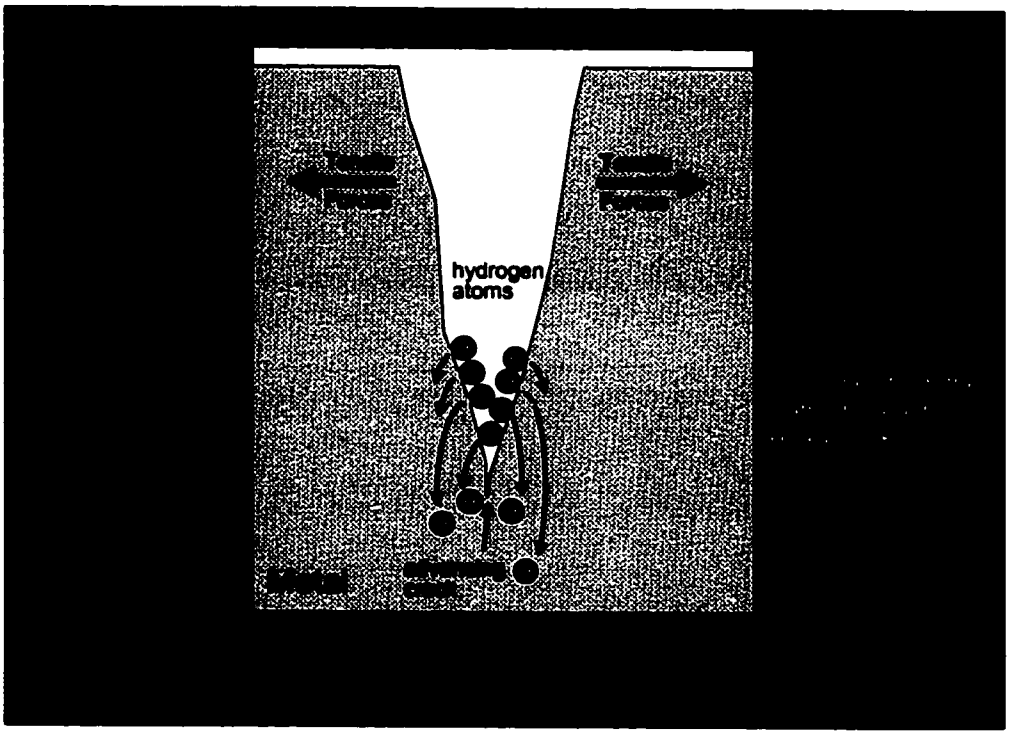

Figure 1.2. Sulfide Stress Cracking

1.3.2 Effect of the Alloying Elements

The microstructure developed after a welding process is an important factor in cracking. It may influence both crack initiation and crack propagation. The microstructure of DMWs can develop a crack-susceptible matrix in which an additional factor, like hydrogen, can operate with destructive results. Actually the dilution of the filler metal with the base metal, producing a distinct intermediate region at the deposit/parent metal interface, and this region may have a significant influence on the qualities of weldment [6].

Alloying elements, the metallurgical conditions, play a major role in SSC of DMWs. This is why the selection of a suitable filler metal is an important consideration in the fusion welding of DMW.

For example Nickel-alloy filler metals are often recommended for DMWs, because the nickel provides a more favorable match between the thermal coefficients of the austenitic and ferritic materials. It also significantly reduces carbon transfer from the ferritic steel [7].

On the other hand, the microstructure of DMWs is significantly affected by carbon migration across the weld interface. Carbon migration causes loss of strength in the ferritic material adjacent to the weld interface and an increase in the hardness in the carbon enriched zone. These zones are immediately adjacent to one another and provide a significant change in properties across a narrow region [7, 8]. It is believed that martensite could form in such a region along the fusion boundary of carbon/stainless steel

welds and increases the hydrogen embrittlement susceptibility of the weldment. The problem becomes more critical when the component is used in an aggressive environments where H_2S is present.

1.3.3 Effect of Stresses

As mentioned above, cracking cannot occur in the absence of stress, regardless of the microstructure and/or its condition. For cracking to occur, the stress imposed on the various microstructural regions by weldment loading must exceed the stress tolerance of the microstructure in one of the regions. The stresses and strains attendant with the production and use of DMWs arise from difference in expansion coefficients of the base metals and filler metals (with the greatest difference being evident for stainless steel filler metals and ferritic base metals), internal and external loading, and from joint configuration [8].

1.3.4 Effect of Preheating

Preheating process involves welding on plates that have been heated to an elevated temperature. This result in a reduction in the cooling rates thereby lowering the temperature gradient. Using the optimum preheat temperature is expected to reduce the extent of the hard zone formation and lower hardness level and hence reduce the susceptibility to SSC. According to Omar [9-10] the use of preheat lowers the cooling rates in the weld metal and in the heat affected zone. This result in a more ductile metallurgical structure that will resist weld cracking. It is logical to serarch for optimum

preheat conditions which will susbtantially slow the weld metal cooling rate and enhance the resistance of weld to SSC.

1.4 Study Objective

This applied research study aims at assessing the susceptibility to sulfide stress cracking of dissimilar metal weld specimens fabricated with different preheat temperatures and different welding electrodes (filler metals) and exposed to a sour service environment.

In order to achieve the objectives of the proposed applied research study, the tasks outlined below were performed:

Task 1 : Survey Of The Literature

A literature review of sulfide stress cracking in dissimilar metal welds was carried out. Case histories of relevant industry and Saudi Aramco experience were reviewed.

Task 2 : Sample Preparation

Test samples were prepared from AISI 316L SS welded to API 5L X60 carbon steel using two filler metals namely, E 309 and Inco 182, and four different preheat temperatures as indicated in Chapter 3. The joint type was Butt joint, the weld type was V groove (single), and the welding process was Shielded Metal Arc Weld.

A number of tensile specimens were prepared for the NACE SSC test in accordance with the exprimental study outlined in Chapter 3. Metallographic examination samples were used for the meatllographic examination, and the EDS & Microhardness surveys.

Task 3 : Mechanical Properties Determination

The actual yield strength of DMW specimens as well as the ductility (elongation and reduction in area) was first determined. These values were used for the SSC susceptibility test outlined below in task 4.

Task 4 : Sulfide Stress Cracking Susceptibility Tests

Sulfide stress cracking susceptibility tests were conducted as per NACE TM 01-77-96 method A. The test solution (5 wt % NaCl and 0.5 wt % glacial acetic acid in distilled water) was deaerated for over 2 hours by purging with nitrogen gas. A continous flow of H_2S was maintained throughout the test duration of 30 days at a rate of a few bubbles per minute. The tests were conducted at different applied loads ranging from 60% to 110% of the Y.S. values.

Task 5 : Metallographic and SEM Characterization

Optical metallography examination of the samples obtained from each welded DMW plate was carried out to examine the microstructure of the critical areas of DMWs. SEM fractography of the fractured specimen was under taken to determine the modes of failure.

Task 6 : EDS and Microhardness Surveys

Energy Dispersive X-Ray Spectrometry (EDS) and Microhardness surveys were also performed to confirmer the finding of previous analysis.

Task 7 : Data Analysis and Conclusion

The experimental data generated in Tasks 3-6 was analysed to gain an insight into the susceptibility of DMW specimens to SSC. Some models were devloped to characterize the level of applied stress and time to failure of the exposed specimemn.

CHAPTER 2

LITERATURE SURVEY

The problem inherent with dissimilar metal weld joints have long been recognized and worked on. However, only few studies have been devoted to investigate sulfide stress cracking of these joints. In the following survey of literature, several studies geared towords understanding and overcoming the problem of SSC, are highlighted.

Lundin [8] in his review article covered the open literature from 1935 to 1982, noted that the majority of failures in DMWs have been associated with austenitic stainless steel filler metal joints compared to the Nickel-based filler metal welds.

Some of the general facts drawn from his survey are as follows:

- Failures occur almost invariably in the Heat Affect Zone (HAZ) of the ferritic component adjacent to the weld metal interface.
- The constituents at the weld interface are difficult to identify, and the precise role of the hard constituents is not well understood.

Elboujdaini et al [4] defined the effect of hardness on SSC behavior of C/Mn and 2.25 CrMo steels in acidified saline solutions. Specimens were loaded using 2 different stresses 90%, and 110% of the yield strength. The test duration was 720 hrs as specified

by NACE standard, TM 01-77, using the four-point bending SSC test method. In addtion to other conclusions attained from the study, it was noted that hardness is a primary factor in controlling the SSC resistance of steels, and HV 248 (HRC 22), according to NACE MR 01-75 standard is a very good safe criteria. No cracks were detected in any region (the base metal, the weld metal, or the heat affected zone) where the hardness was below HV 260 for all of the different kinds of welds studied.

Catastrophic SSC failure of a dissimilar metal weld in a high pressure hydrogen vessel made of 3 ½ Ni steel was reported by Craig and Setterlund [12]. Sulfide stress cracking tests were conducted using specimens from the longitudinal sumerged arc weldment. Cracks and failure mode were detected on almost all samples similar to those observed in the heat exchanger. Failure was attributed to SSC of the fusion line that developed after welding the 3-1/2 Ni steel plate with an austenitic stainless steel filler metal.

Metallographic examination revealed that the fracture originated in the weld root along the fusion line but the fracture propagated in a region approximately 0.0001 to 0.0004 inches away in the base metal. A close-up examination of the fusion line revealed a feathery microstructure typical of martensite and a high concentration of carbides. A microhardeness traverse from the weld through the HAZ indicated the existence of a hard dark-etching zone along the weld line having a hardness of significantly greater than either the weld or the base metal. The hardness of this dark-etching zone was equivalent to HRC 30. The ferrite band, on the other hand, had an equivalent hardness of only HRB 75, lower than either the weld or base metal harnesses.

In another study done by the Research Institute of King Fahd University of Petroleum and Minerals, dissimilar metal welds (DMWs), 316L stainless steel welded to Carbon Steel using five different filler electrodes (E-7018 carbon steel, 309 stainless steel, Inco 182, Inco 625, and 309-Mo) were tested using the slow strain rate method [13].

The study objective was to study the SSC susceptibility of dissimilar metal welds. The tests were conducted in an aqueous environment containing Cl^-, HCO_3^-, and SO_4^-. And the solution was in contact with a gaseous mixture of H_2, H_2S, CO_2, CH_4, and N_2.

The study concluded that all five dissimilar metal couples tested were susceptible to SSC. And the susceptibility of DMW to SSC is dependent on the type of galvanic couple created by the welding electrode. Failure was also attributed to the hardness and the test temperature.

All samples experienced severe loss in ductility due to hydrogen-assisted cracking. In the order of highest to lowest susceptibility to SSC, the five electrodes tested were arranged as follow: 309, E-7018, 309-Mo, I-625, I-182.

The sulfide stress corrosion cracking susceptibility of 5 different Fe-Mn-Al weld metals in addition to 310 and 316 conventional stainless steel weld metals were examined by Makhamreh and Aidun [14]. Fe-Mn-Al and Fe-Cr-Ni weld metals were prepared using the flux cord arc welding process.

The constant load stress corrosion cracking test in acidic aqueous solution saturated with H_2S gas (NACE solution) revealed that the Fe-Mn-Al electrods performed better than the 310 and 316 electrods in resisting cracking in NACE solution. Another important conclusion was that the susceptibility to stress corrosion cracking of Fe-Mn-Al

weld metals in NACE solution can be related to the strength (or hardness) of these weld metals. The resistance to stress corrosion cracking (higher strength at longer times) increased as the hardness of the Fe-Mn-Al weld metals decreased.

Onsqien et al [15] investigated the specific effects of microstructure on SSC susceptibility of low-carbon steel weldment. They found that the formation of marensite give rise to a substantial decrease in the SSC resistance. They also concluded that the resistance to SSC can be significantly improved by a decrease in cooling rate.

Doody [1], emphasised that the problem area of DMWs is the fusion line region on the carbon steel side of the joint, where there exist very small hard zones. These small intermediate mixed zones (IMZs) are of intermediate composition between the carbon steel base metal and the bulk weld metal composition. They are very thin, non-continuous layers, with a hard microstructure. For DMWs, the formation of such localized hard areas is a concern for possible initiation of sulfide stress cracking. This is based on two well documented items in the literature. First, a microstructure of untempered martensite is highly susceptible to any form of hydrogen cracking, including sulfide stress cracking. Second, subsurface hard areas can initiate cracking in wet sour service.

Chan et al examined the mechanical behavior of DMW in H_2S charging environment [6]. Different filler metals (E7018, E308, EniCrFe-2) were selected to weld mild steel (SM41A) and austenitic stainless steel (type 304SS). Both the constant slow extension rate tensile testing and the constant load rupture tests of these weldements were carried out in H_2S saturated NACE solution. The researchers concluded that the intermediate region adjacent to the fusion boundary, which exhibits the most significant

variations in composition, may suffer hydrogen embrittlement in H_2S saturated solution. And the extent of martensite formation plays major factor in the susceptibility to hydrogen embrittlement.

In another work done on welded joints of low alloy steel, Poepperling et al [16] concluded that in weldements with maximum hardness values below 350 HV10, the cracks do not occur in the hardest region of the HAZ but in the regions of softer microstructures. Only at hardness values in excess of 350 HV10 do the location of maximum hardness and the fracture coincide.

Wortel addressed the behavior of ferritic/austenitic dissimilar welded joints [17]. In his study he concluded that:

- The susceptibility to H_2S stress corrosion cracking in the Local Hard Zones (LHZ) can be strongly reduced by avoiding a wide continuous LHZ. This can be achieved with Ni-base consumables instead of Fe based austenitic consumables.

- The width of LHZ is key factor for hydrogen service. A small discontinuous width is preferable. The type of electrods and the heat-treatment conditions predominantly determines the width.

In supporting the positive effect of the pre-heating process, Omar of Saudi Aramco, conducted two studies [9-10] in which he verified the use of preheating process as a method of reducing the extent of hard zone formation and lowering hardness level. This was evident in joints fabricated with Inco 182 electrodes. Omar [9] also discussed the defects along with the effects of welding electrodes, welding processes, buttering and postweld heat treatment (PWHT) on the formation of localized structure in welded dissimilar metals. Test results showed that the extent of hard zone formation in full

penetration butt-welds of dissimilar metal joints fabricated with EniCrFe-3 (Inco 182) welding electrode was much less than those fabricated with E 309 austenitic stainless steel electrode. Nevertheless, hard zones of welds fabricated with either electrode still exhibited hardness levels that exceeded VHN 300. Although some reduction in the hardness level of joints fabricated with carbon steel and Inco 182 electrodes was experienced at the higher PWHT temperatures, the hardness level of most PWHT'd welds were still well above VHN 250.

In a second study, Omar [10] tried to determine the optimum welding conditions which when correctly applied, will drastically reduce or totally eliminate formation of localized hard structure in DMWs. Omar's results which were presented at the American Welding Society (AWS) Technical Conference in April' 1996, are displayed in Figures 2.1 and 2.2.

In summary, the following general conclusion may be drawn from the litrature.

1. Formation of the hard zones in DMWs, regardless of the type of the base metal and/or the electrode, is difficult to avoid.
2. The constituents at the weld interface are difficult to identify, and the precise role of the hard zones is unclear.
3. However, the extent of the hard zones formation can be drastically reduced by the optimum preheat.
4. The hard zones adjacent to the fusion boundary may suffer hydrogen embrittlement in H_2S saturated solution. The extent of martensite formation plays a major factor in the susceptibility of DMWs to hydrogen embrittlement.
5. The higher the hardness of DMW, the higher its susceptibility to SSC.

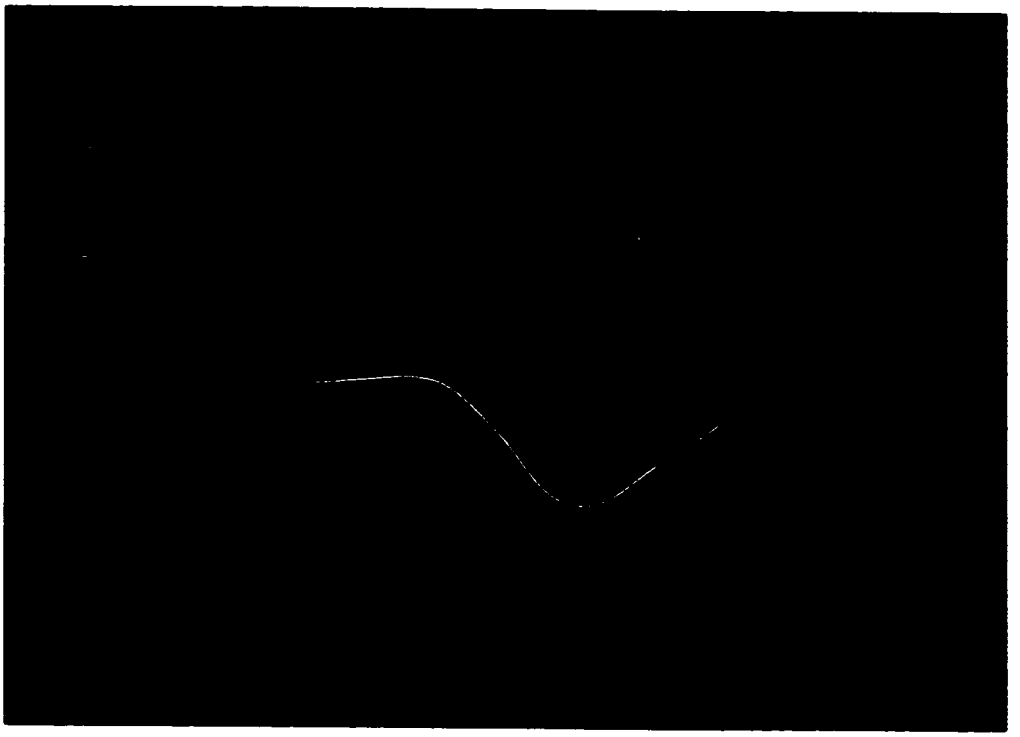

Figure 2.1. Preheat temperature vs. hard zone length [10].

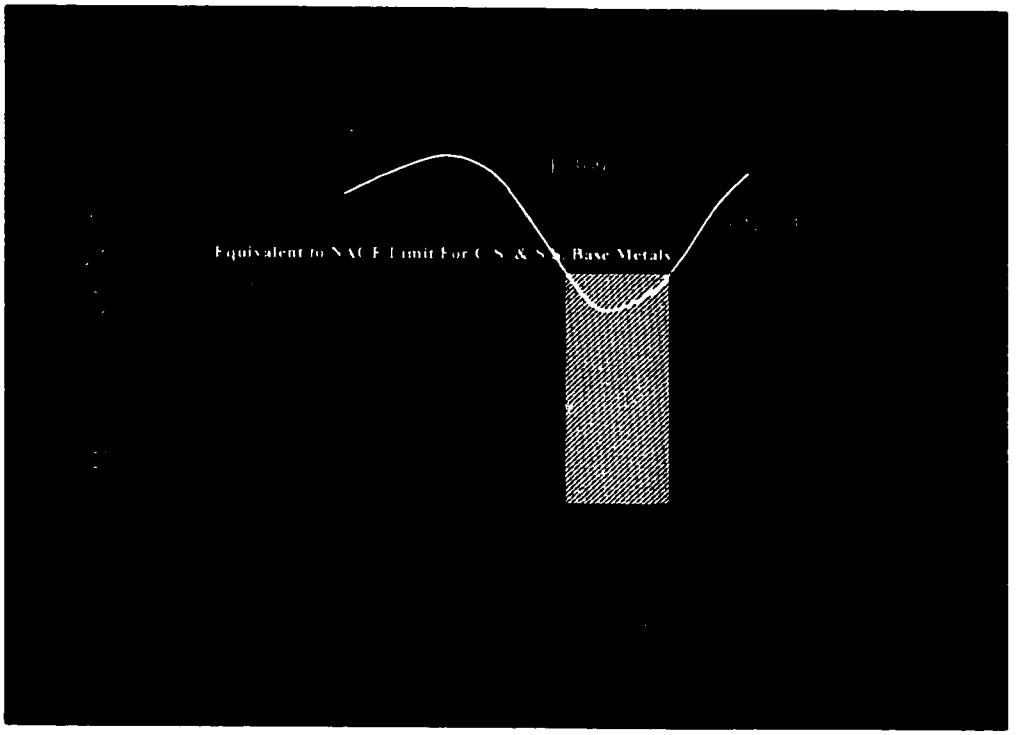

Figure 2.2. Preheat temperature vs. hardness level [10].

CHAPTER 3

EXPERIMENTAL PROCEDURE

3.1 Welded Plates Preparation

A total of 8 API 5L X60 Carbon Steel plates were welded to AISI 316L plates (see figure 3.1 & 3.2) using two different electrodes: E 309 SS, and Inco 182 (ENiCrFe-3). The dimensions of each plate were: 1/2" (12.7 mm) X 4" (101.6 mm) X 18" (457.2 mm) (T X W X L) minimum.

DMWs plates were joined according to the following design, material, and process parameters:

- Joint Design — Full penetration single V groove butt, with 60 degrees inclined angel, 1/16" root face, and (3/32"-1/8") root opening.
- Welding Process — Manual Shielded Metal Arc Weld (SMAW).
- Welding Electrodes — 1/8" (3.2 mm) dia. E 309 and Inco 182 (ENiCrFe-3).
- Preheat Temperature — 350, 400, and 450°F (177, 205, and 232°C) maintained throughout welding. This is in addition to two plates in the no preheat condition used as control plate.

Table 3.1 lists the various preheat treatment, and electrods under which the above mentioned 8 DMWs plates were prepared. The material composition of both metal plates and the filler metals was determined and are given in Table 3.2. The DMW plates were radiographed after weldeing to check for welding defects. Figure 3.1 shows a drawing of the DMW plate 'fit-up', and Figure 3.2 is a photograph of one of the welded plates.

Table 3.1. Eight DMW combinations with their corresponding electrode and preheat treatment

Weld No.	DMW Combination			Preheat Treatment
	Base Metal	Weld Metal (Electrode)	Base Metal	
1	API 5L X60 CS	E309 SS	AISI 316L	None
2	API 5L X60 CS	E309 SS	AISI 316L	350°F
3	API 5L X60 CS	E309 SS	AISI 316L	400°F
4	API 5L X60 CS	E309 SS	AISI 316L	450°F
5	API 5L X60 CS	Inco 182	AISI 316L	None
6	API 5L X60 CS	Inco 182	AISI 316L	350°F
7	API 5L X60 CS	Inco 182	AISI 316L	400°F
8	API 5L X60 CS	Inco 182	AISI 316L	450°F

Table 3.2. Chemical composition of the base and filler metals

Chemical Composition of the ASIA 316L Base Metal	
Element	*wt %*
Fe, Iron	66.45
C, Carbon	0.035
Si, Silicon	0.44
Mn, Manganese	1.21
Cr, Chromium	17.33
Ni, Nickel	11.9
Mo, Molybdenum	1.98
Cu, Copper	0.26
Ti, Titanium	0.0043
Nb, Niobium	0.043
Al, Aluminium	0.005
V, Vanadium	0.041
W, Tungsten	0.049
S, Sulphur	0.0069
P, Phosphorus	0.03
Co, Cobalt	0.22

Chemical Composition of the C.S. API 5L X60 Base Metal	
Element	*wt %*
Fe, Iron	98.11
C, Carbon	0.052
Si, Silicon	0.3
Mn, Manganese	0.93
Cr, Chromium	0.0033
Ni, Nickel	0.07
Mo, Molybdenum	0.11
Cu, Copper	0.16
Ti, Titanium	0.051
Nb, Niobium	0.079
Al, Aluminium	0.032
V, Vanadium	0.02
W, Tungsten	0.049
S, Sulphur	0.011
P, Phosphorus	0.023
B, Boron	< 0.0005

Chemical Composition of the E 309 Filler Metal	
Element	*wt %*
C	0.12
Cr	24
Ni	13
Fe	57
Mo	2.5
Mn	1.5
Si	0.5

Chemical Composition of the Inco 182 Filler Metal	
Element	*wt %*
C	0.05
Cr	15
Ni	63
Fe	10
Mn	7
Si	0.5
Nb	1.75

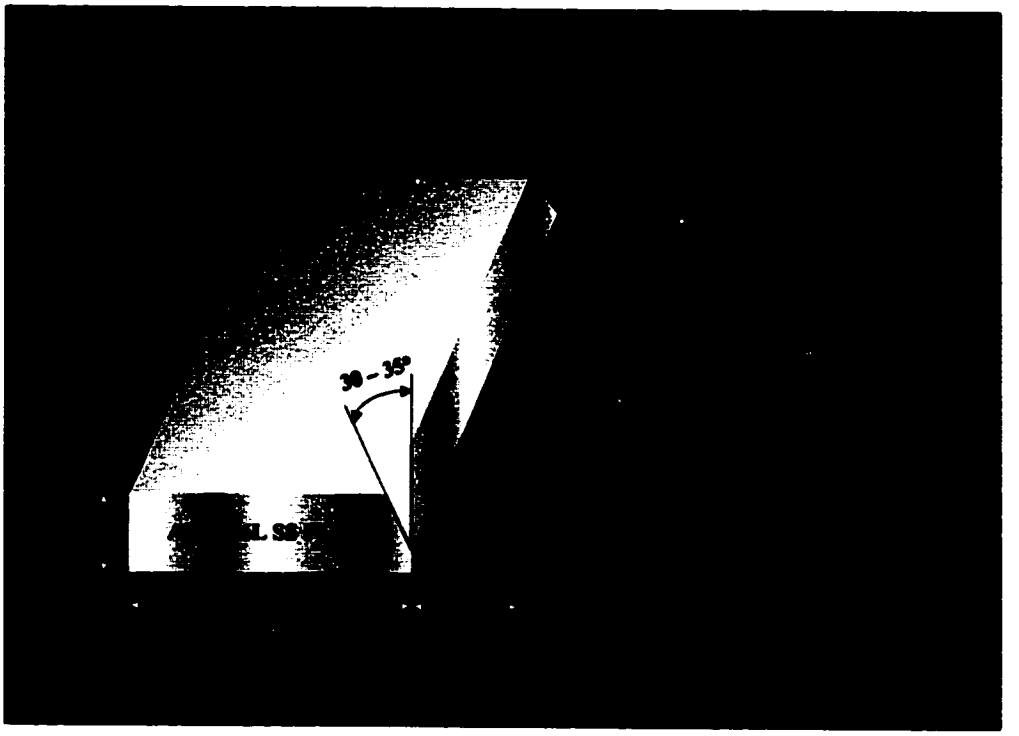

Figure 3.1. DMW plate fit-up

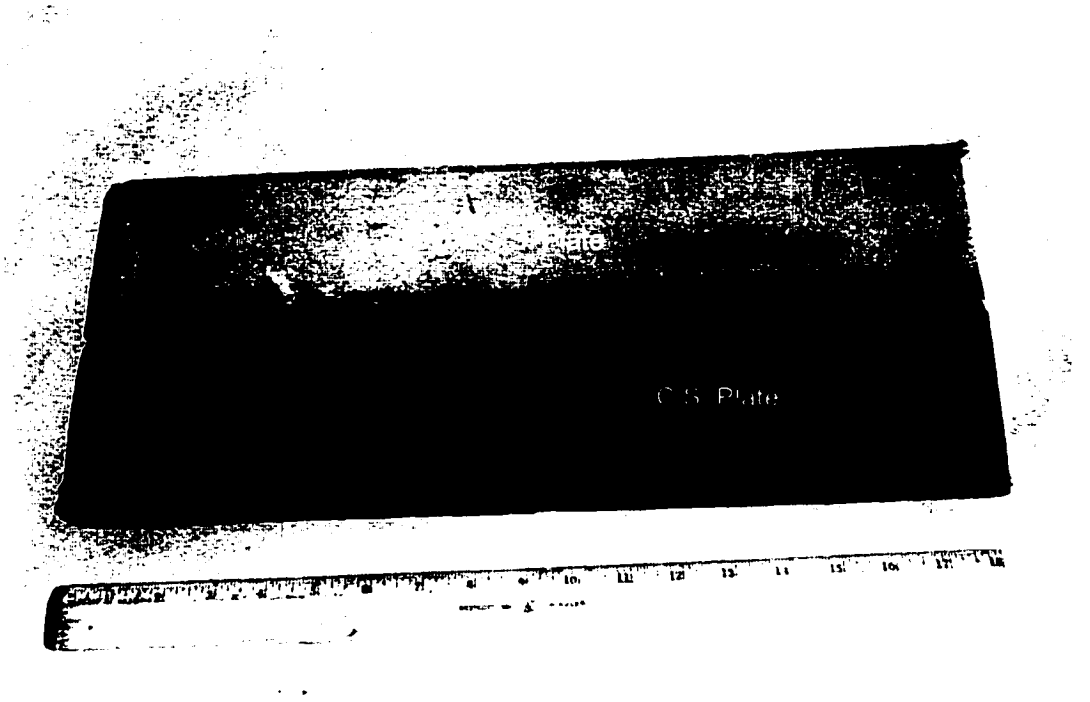

Figure 3.2. Photogrph of one of the DMW plates.

3.2 Sample Preparation

From each DMW plate the following specimens were prepared:

1. Three rectangular specimens for metallographic examination were prepared. Samples were taken from the top, center, and bottom positions of each DMW plate. These specimens were first sectioned and metallographical samples prepared by mounting them in Bakelite. The mounted samples were polished using Silicon Carbide paper down to 600 grit followed by diamond polishing down to 1μm, and final polish using Alumina powder (0.3μm). The polished samples were then etched with either 5% nital to reveal the carbon steel section, or electrolytical etched using 10% oxalic acid for the stainless steel. Microscopic examination of these (8 X 3 = 24) specimens was then conducted in order to determine the extent of hard zone formation. Figure 3.3 is a schematic sketch for the cutting postions for all samples.

2. Two round tensile specimens of 0.25" (6.35 mm) diameter and 1" (25.4 mm) gauge length were machined (from each plate) for mechanical properties determination according to ASTM A370 (see Figure 3.4). 0.2% offset yield strength, elongation, and percent reduction in area were determined. The standard tension specimen and the SSC test specimen were machined in the same orientation such that variation in the properties that normally occur from specimen to specimen is minimized. Thus a total of 2 X 8 = 16 specimens were preapred for this test.

3. Nine tensile specimens from each plate as per NACE TM 01-77-96 method A were prepared for the NACE SSC tension test (3 samples loaded at 110% Y.S., 3 at 80%

Y.S., and 3 at 60% Y.S.). Thus a total of 9 X 8 = 72 specimens were prepared for this purpose.

The number of tensile samples required for this test program is as follow:

- Samples needed for the evaluation of the Mechanical Properties (see task 3): 2 samples per treatment X 4 treatments X 2 filler electrodes = 16 samples.

- Samples needed for the TM 01-77-96 test: 9 samples per test* X 4 treatments X 2 filler electrodes = 72 samples (*Samples needed for different level of stress: 3 samples at 110% Y.S., 3 at 80% Y.S., and 3 at 60% Y.S.).

  Thus the total number of samples is: 16 + 72 = 88 samples.

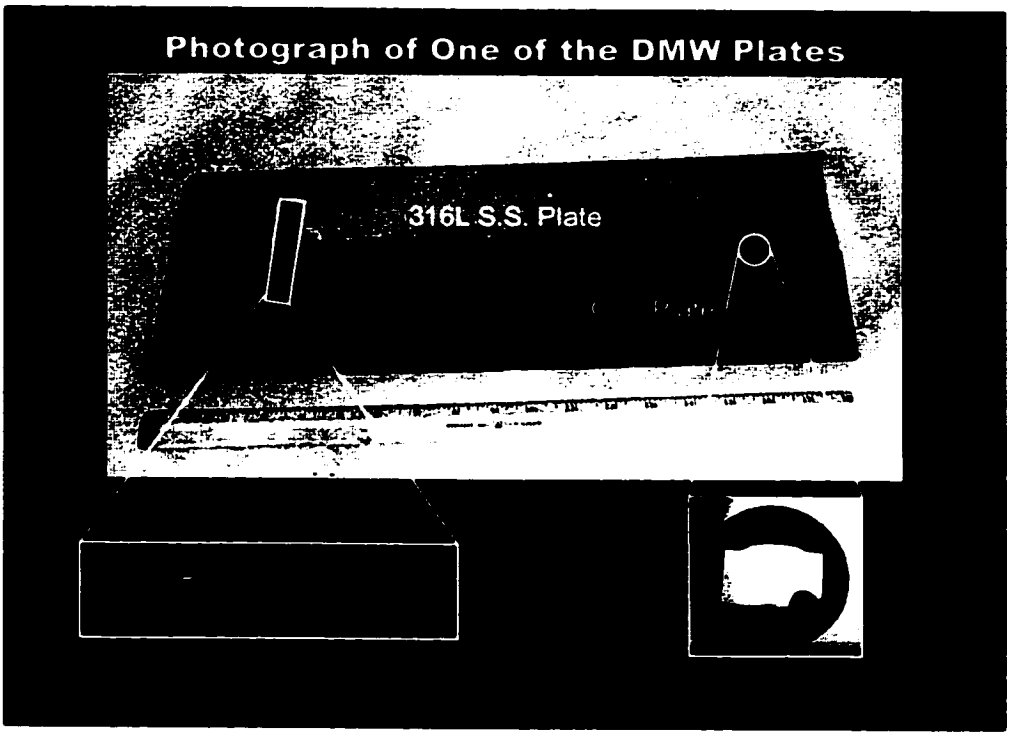

Figure 3.3. Schematic sketch showing the specimens cutting postions.

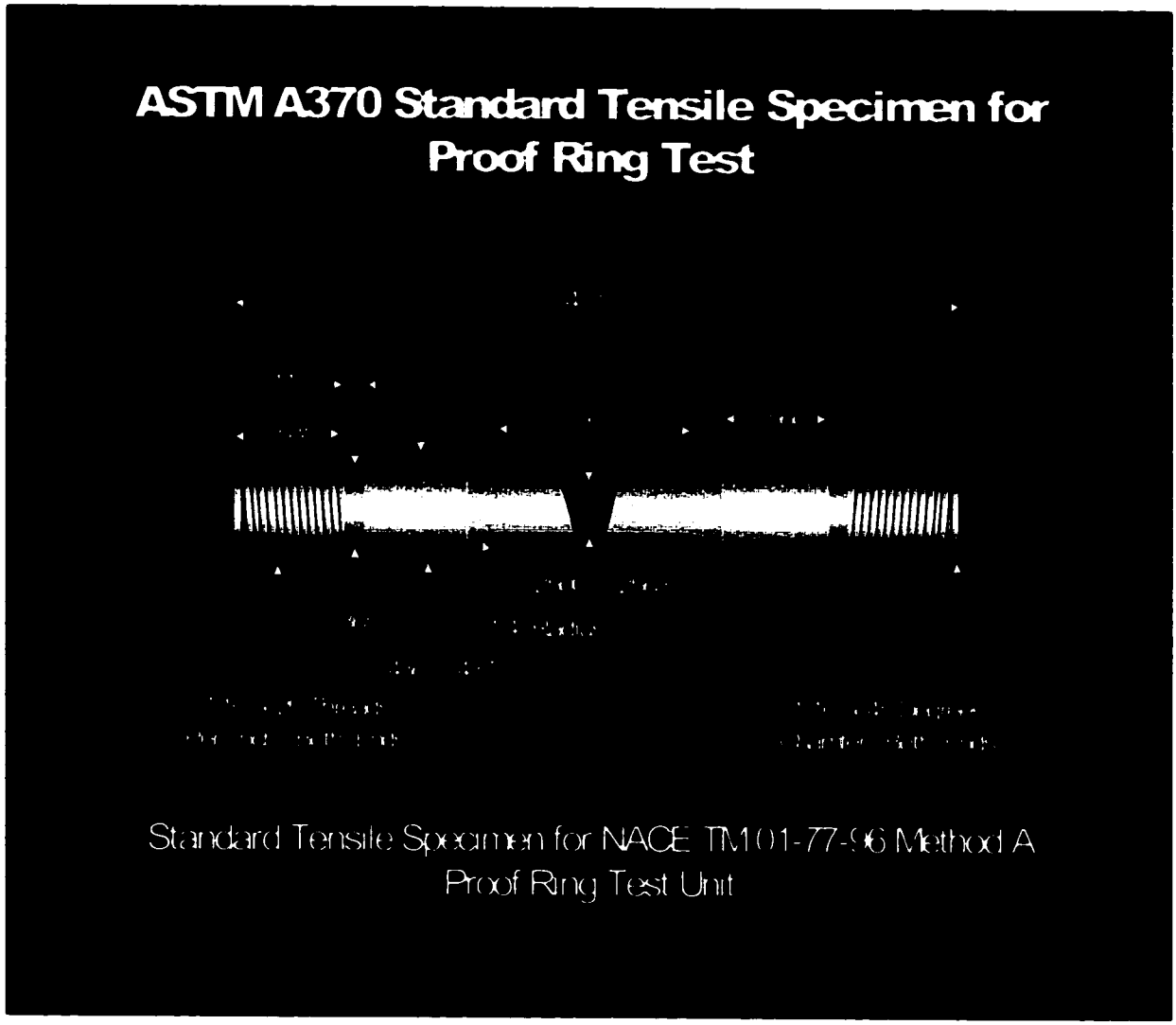

Figure 3.4. ASTM A370 standard tensile specimen for proof ring test.

3.3 Tensile Testing

Tensile testing, according to ASTM A370, was first conducted to determine the yield strength for each DMW combination and for each heat treatment condition. Since the testing was conducted on two (2) samples, the average yield strength values were used to set up the %Y.S. loading increments of the NACE TM 01-77-96, Method A using Proof Rings.

3.4 Sulfide Stress Cracking Susceptibility Tests

3.4.1 Introduction

Sulfide stress cracking susceptibility tests were conducted as per NACE TM 01-77-96 method A. This test method was originally issued in July 1977, and as the test method was put into practice in many laboratories, additional information was gained as to the factors affecting the results. In March 1980, it was revised to include this experience. The revised test method was issued in January 1986. The latest revision was in 1996.

The NACE Standard Tensile Test aids in the evaluation and selection of all types of metals and alloys, regardless of their form or application, for service in H_2S environments. It is directed primarly toward the testing of metals subjected to tensile stress for resistance to cracking failure in low pH aqueous environments containing H_2S.

The determination of SSC susceptibility with this tensile test method is usually based on time-to-failure, where tensile specimens loaded to a particular stress level will

give a fail/no-fail test result. When multiple specimens are tested at varying stress levels, an apparent threshold stress level for the occurrence of SSC can be obtained.

3.4.2 Test Equipment

Tension tests were performed with sustained load devices (proof rings, ASTM G49-76, Figure 3.5). Testing with constant load device ensures that susceptible materials will fail completely, eliminating the chance that a small crack will be overlooked in visual and microscopic examination of the test specimens.

A substantial decrease in the proving ring deflection may signify one of the following:

(1) The initiation and propagation of cracks in the specimen,

(2) Yielding of the specimen, or

(3) Relaxation of stress.

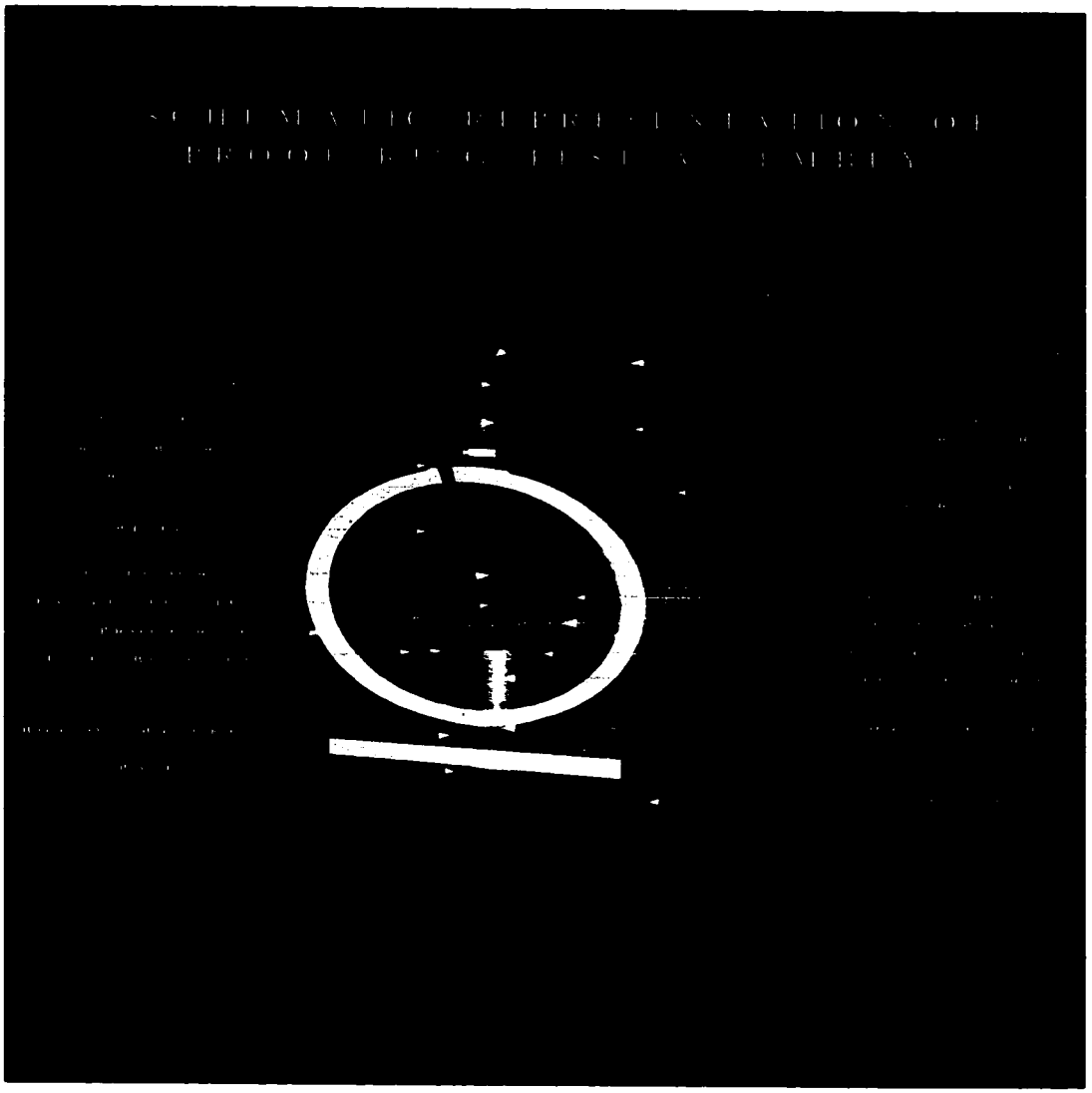

Figure 3.5. Description and important parts of the proof ring unit.

All loading devices were calibrated to ensure accurate application of load to the specimen. The loading devices are constructed in such a manner that torsional loads are avoided. The assembled test cell is shown in Figure 3.6.

The test vessels are capable of being purged to remove oxygen before the test is begun and also capable of keeping air out during the test. The use of a small outlet trap on the H_2S effluent line, to maintain 1.0 inch (25.4 mm) of water back pressure on the test vessel, helped in preventing oxygen entry through small leaks or by diffusion up the vent line.

Load levels for stressing tensile specimens was based on the cross-sectional area of the specimen based on the following equation:

$P = Y.S. \times A$; where: P = load, Y.S. = Yield Strength of the material,

and A = actual cross-sectional area of the gauge section.

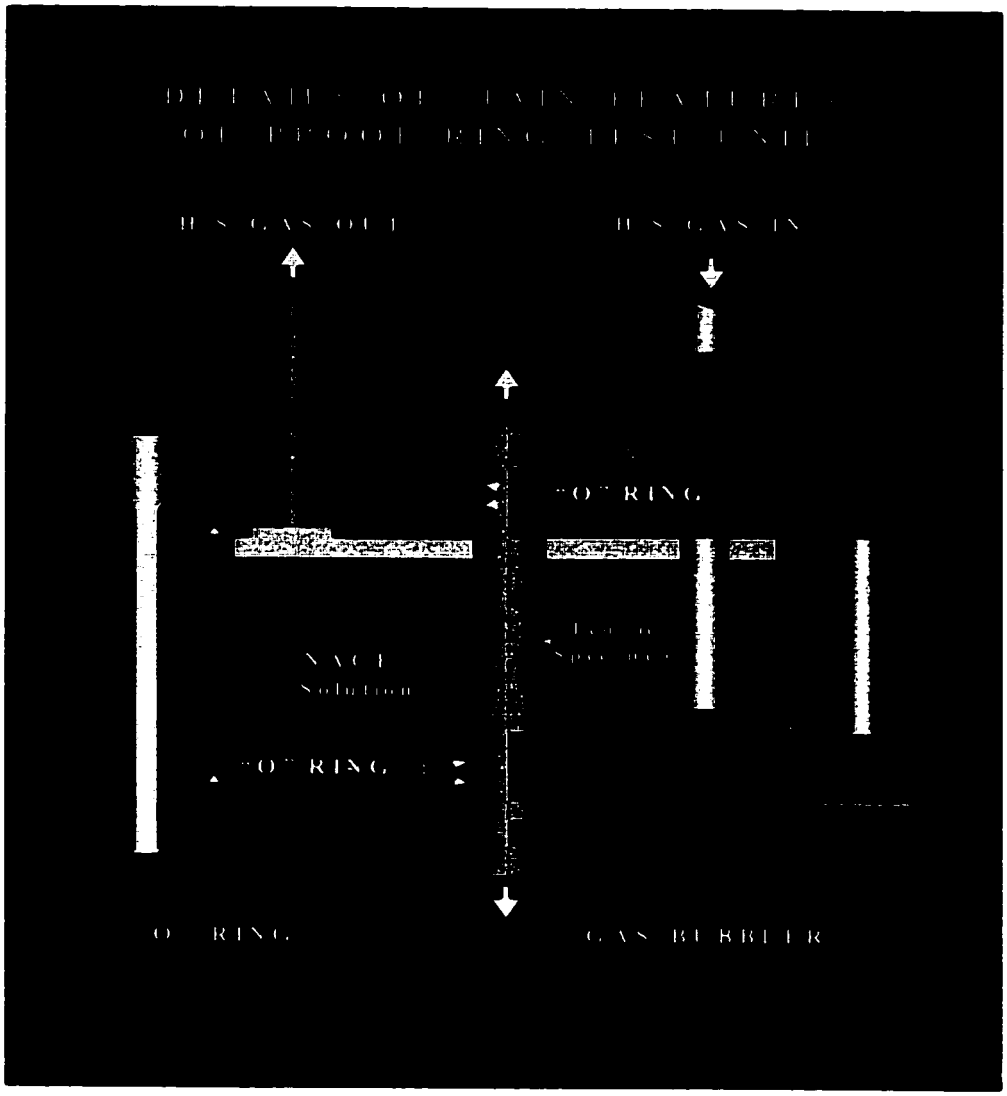

Figure 3.6. Tensile specimen assembled in the test cell.

3.4.3 Test Solution

The test solution for the Standard NACE tensile test is an acidified, H_2S-saturated aqueous environment. It consists of 5.0 wt.% NaCl and 0.5 wt.% glacial acetic acid in distilled water. The initial pH was approximately 2.7, and may increase during the test but shall not exceed 4.0.

The solution was deaerated for over 2 hours by purging with nitrogen (N_2) gas before H_2S was introduced. A continuous flow of H_2S was maintained throughout the test duration of 30 days at a rate of a few bubbles per minute at a temperature of 75±5°F (24±3°C).

The gases, sodium chloride, acetic acid, and solvents are all reagent or chemically pure, 99.5% minimum purity. The water was distilled and of quality equal to or greater than ASTM Type IV (ASTM D193). For this test method, the inert gas used for removal of oxygen was high purity nitrogen.

3.4.4 Test Specimen

Tensile specimens as per NACE TM 01-77-96 method A were prepared for the NACE tension test. The gauge section of the tension specimen (Figure 3.4) was 0.25 inch (6.35 mm) in diameter and 1.0 inch (25.4 mm) long (ASTM A370). The radius of curvature at the ends of the gauge sections was at least 0.25 inch (6.35 mm) to minimize stress concentrations and fillet failures. Ends of the specimen were long enough to accommodate seals for the test container and to make connections to the stressing fixture (Figure 3.6). Machining of the specimens was done carefully to avoid overheating and

cold working in the gauge section. In Machining operations, the final two passes were such that no more than a total of 0.002 inches (0.05 mm) of material was removed. The specimen was finished to a surface roughness of 32μin (0.81μm) or finer. After machining, specimens were stored in a desiccator until ready for testing.

3.4.5 Testing Sequence

1. The minimum gauge diameter of the specimen was measured and the specimen load for desired stress level was calculated.
2. The tensile testing specimens were degreased with 1,1,1-trichloroethane in an ultrasonic cleaner and later rinsed with acetone. The gauge sections of the specimens were handled property and were not contaminated after cleaning. After which the specimens were placed in the test cell.
3. The test cell was sealed after placing the specimen to prevent leaks of air into the cell during the test.
4. The load was applied before the test cell was purged with inert gas. The load was carefully applied, taking care not to exceed the desired level of loading. If the desired load was exceeded, the test was discarded.
5. The test cell was immediately filled with dearated solution. Deaerated solution was prepared in a sealed vessel that was purged with inert gas (N_2) at a rate of at least 100 ml/min. for at least one hour per liter of solution.
6. The solution, once in the test cell, was purged again with inert gas for at least 30 minutes. The purpose of this was to ensure that the test solution was essentially oxygen-free prior to the introduction of H_2S. Oxygen contamination is evident by a cloudy (opaque) appearance in the solution where the H_2S gas was admitted to the test cell. An opaque appearance to the test solution upon admission of H_2S was deeming to disqualify the test.

7. The solution was then saturated with H_2S at a rate of 100 to 200 ml/min for 20 minutes per liter of solution. It is necessary to maintain a continuous flow of H_2S through the test container and outlet trap for the duration of the test at a low flow rate (a few bubbles per minute). This maintains the H_2S concentration and a slight positive pressure to prevent air from entering the test container through small leaks. H_2S gas was continuously purged at a low flow rate throughout the test duration.

3.4.6 Application of Constant Loads Sequence

Application of the constant loads was according to the flowchart shown in Figure 3.7. Selection of the 60%, 80%, and 110% Y.S. strength loads was based on Saudi Aramco experience in designs where the usual practice is to make the designs at 60 to 80% of the yield strength. The 110% Y.S. case is choiced to represent the worst-case scenario.

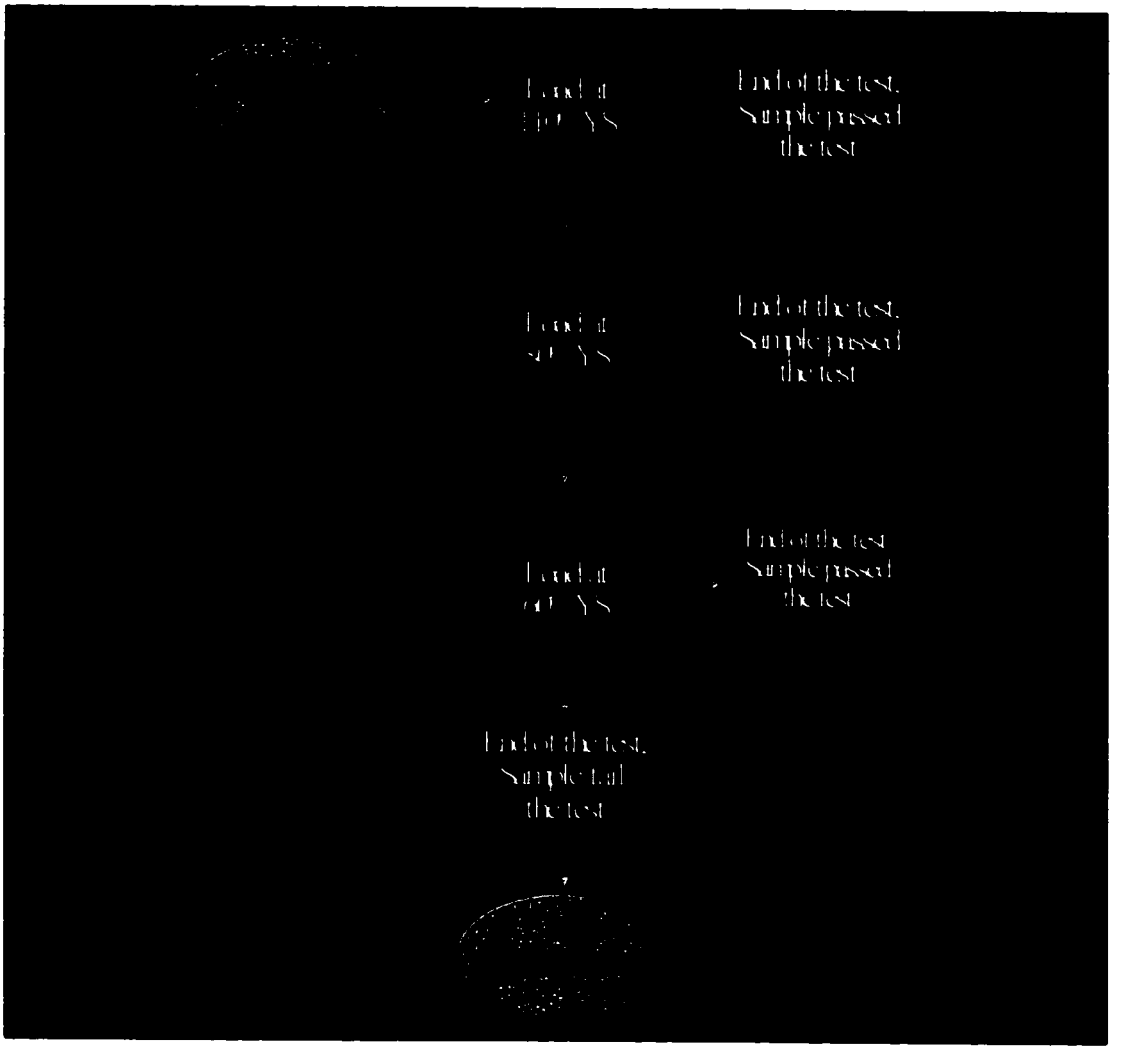

Figure 3.7. SCC Test loading sequence flow chart.

3.4.7 Detection of Time-to-Failure

The termination of the test was at specimen failure or after 720 hours (30 days), which ever occurs first. Failure is defined as the occurrence of complete separation of the specimen. Visual observations of cracking on the gauge section of the specimen at 10X after completion of the 30-day test duration was also considered as a test specimen failure. Consequently, following exposure, the surfaces of the gauge section of the non-failed specimens were cleaned and visually inspected for evidence of cracking. Time-to-failure was recorded using electrical timers equipped with micro switch devices.

The overall setup of the test is shown in Figure 3.8, for six proof rings installed at a time along with gas control module and elapse time monitor (connected with micro switches) to record the time to failure for each sample.

The specimens were electrically isolated from any other metals in contact with the test solution. The seals around the specimens were electrically insulated and airtight and also allowed movement of the specimen with negligible friction.

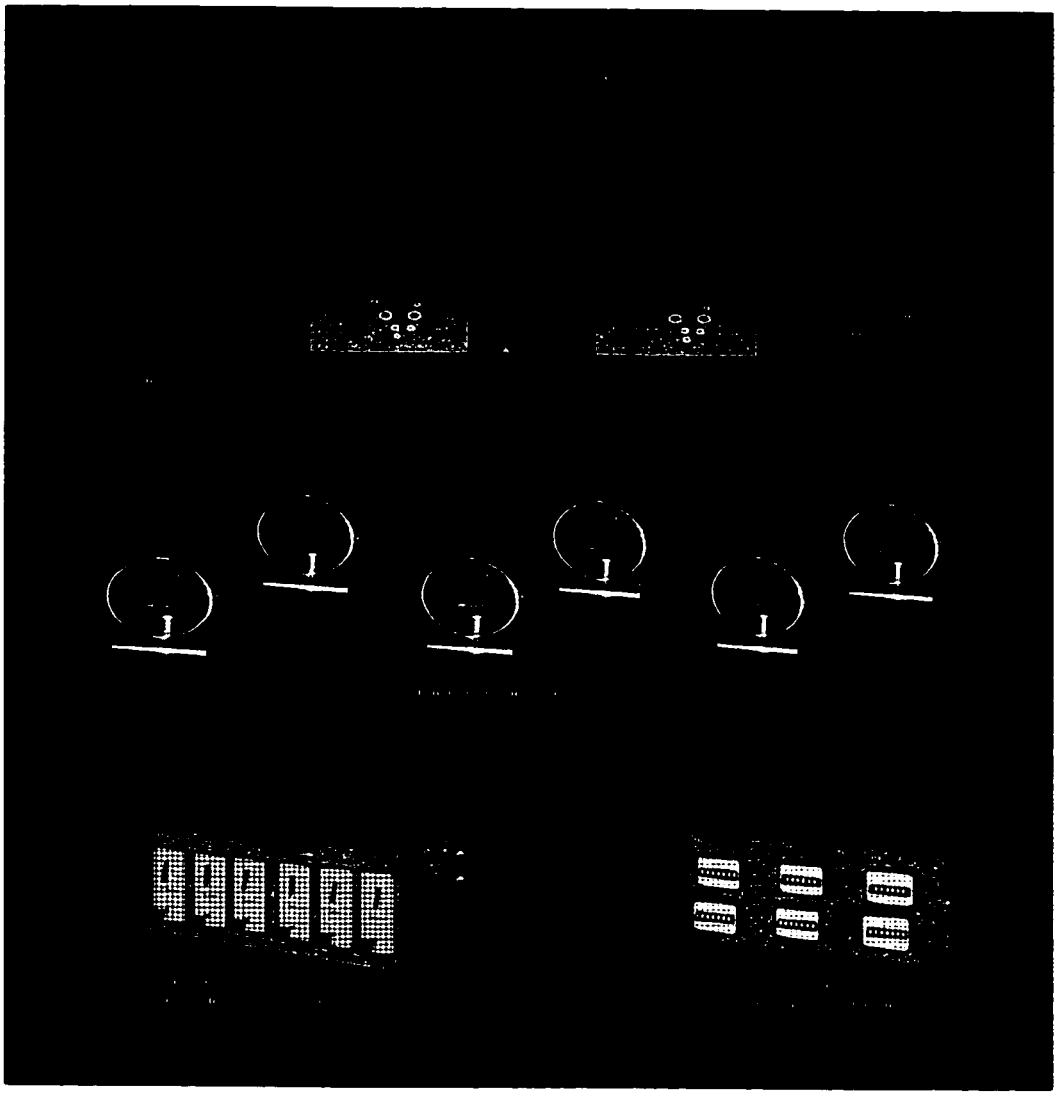

Figure 3.8. Schematic set-up of six proof rings of test.

3.5 Metallographic Examination

Weld cross sectional samples were prepared from each of the welded plates to examine the nature of the fusion boundary transient region and determine the extent of hard zones, both in the as-welded condition (non preheated) and after different preheating treatments.

Both Nital and electrolytic Chromic acid (CrO_3) etching were used alternatively to reveal the weld fusion boundary microstructure as well as the heat-affected zone (HAZ) of the carbon steel base metal. Electrolytic etching, using 10% oxalic acid, was also used to reveal the microstructure of the stainless steel.

3.6 Scanning Electron Microscope Characterization

After NACE testing, selected fracture surfaces of tensile specimens were viewed under the Scanning Electron Microscopy (SEM) to determine nature and features of the crack (i.e. brittle or ductile), and to determine initiation and propagation sites.

3.7 EDS and Microhardnees Surveys

Energy Dispersive X-Ray Spectrometry (EDS) and Microhardness surveys were also performed to confirmer the finding of previous analysis.

CHAPTER 4

RESULTS AND DISCUSSIONS

4.1 Tensile Properties

4.1.1 Effect of Preheat on Yield Strength

The results of yield strength of the transverse tensile specimens taken from each of the welded plates are presented in Table 4.1. The average yield strength value from two (2) specimens prepared from each welded plate was used as the base line Yield Strength of the DMWs in different preheat conditions. There were no significant variations in yield strength values between the two specimens taken from a single weldment. However, there was a slight reduction in the yield strength as the welds preheating temperatures were increased, except at 400°F (205°C) for the Inco 182 welded samples, and at 350°F (177°C) for the E 309 welded samples (the optimum preheat temeprtures for these two weld metals as accroding to Omar [10]), see Table 4.1 and in Figures 4.1 and 4.2.

The decline in the Y.S. values can be explained by the migration of carbon from the ferritic carbon steel material towards the fusion line causing loss of strength in the

ferritic material adjacent to the weld interface and an increase in hardness in the filler metal side. According to Lundine [8], the carbon-denuded zones exhibit low tensile strength.

As noted from Table 4.1, the loss of strength (Y.S. value) is less at the optimum preheat temperatures for both weld metals compare to other two preheat temperatures. It is believed that carbon migration was less at these temperatures.

Table 4.1. Mechanical properties of welded samples before SSC test exposure.

Weld Metal	Welding Condition	Sample 1 Y.S. [Ksi]	Sample 2 Y.S. [Ksi]	Average Y.S. [Ksi]
Inco 182	No Pre-heat	52.13	-	52.13
	350°F Pre-heat	45.7	51.98	48.84
	400°F Pre-heat	56.63	55.01	55.82
	450°F Pre-heat	51.77	45.3	48.535
E-309	No Pre-heat	53.61	-	53.61
	350°F Pre-heat	54.8	58.25	56.525
	400°F Pre-heat	49.62	54.67	52.145
	450°F Pre-heat	48	48	48

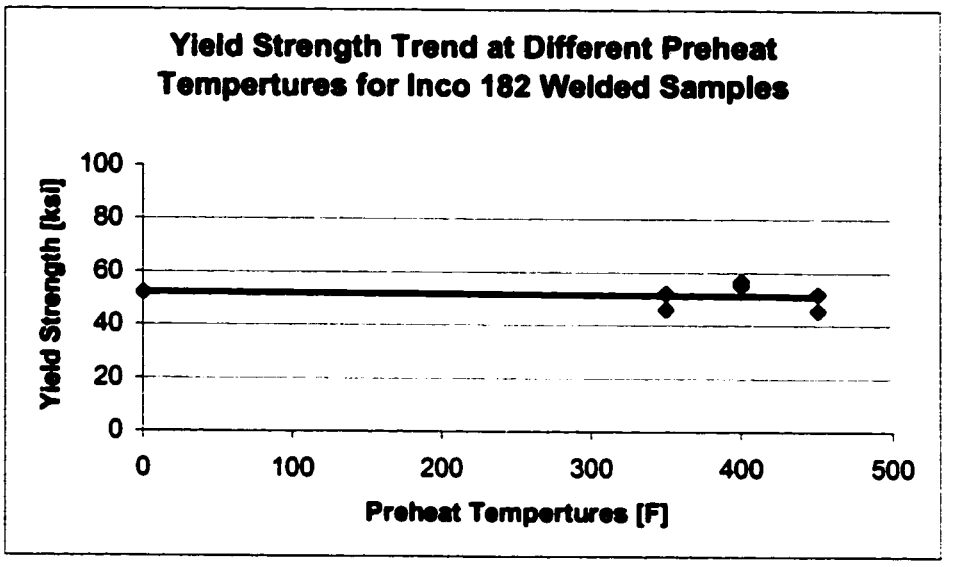

Figure 4.1 Y.S. trend at different preheat temp. for Inco 182 welded samples (specimen not exposed to H_2S).

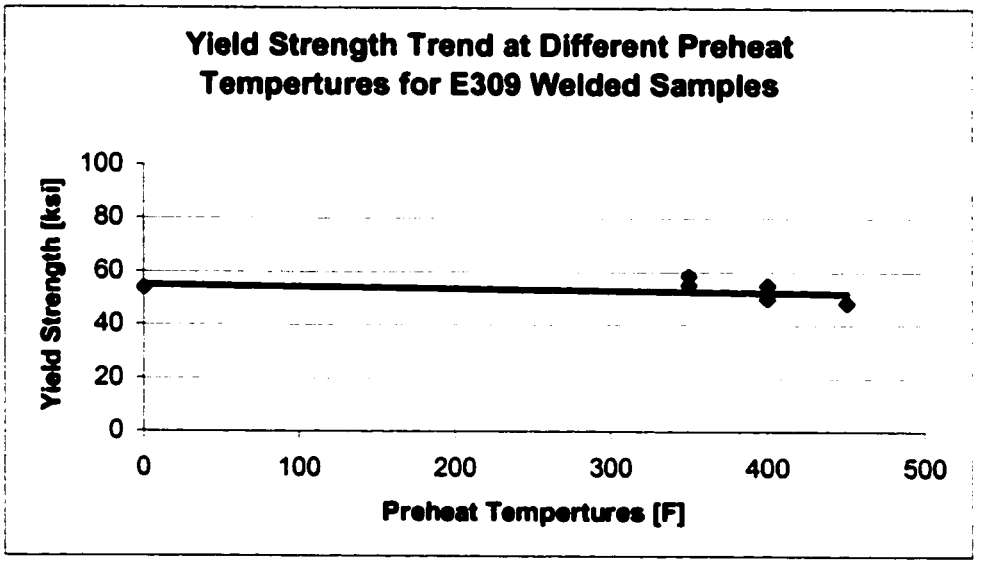

Figure 4.2. Y.S. trend at different preheat temp. for E309 welded samples (specimen not exposed to H_2S).

4.1.2 Ductility Measures at Different Preheat

Table 4.2 lists the remaining mechanical properties (ductility) obtained from the mechanical tensile tests preformed on the transverse samples taken from each of the welded plates. Ductility is the amount of deformation that a material can withstand without breaking, and is measured either as:

- % Elongation = $[l_f - l_0] / l_0 \times 100$, or as
- % Reduction in Area = $[A_0 - A_f] / A_0 \times 100$

where, l_f = the final specimen length; l_0 = the initial specimen length

A_f = the final cross sectional area; A_0 = the initial cross sectional area

Figure 4.3 and Figure 4.4 are graphical representation of the values listed in Table 4.2 where they show slight decline in the ductility for both weld metals with increase in preheating temperature. This indicates that there was not much gain attained from the preheating process in term of ductility.

As it was observed, the effect of preheating on the mechanical properties (both Y.S. and Ductility) is not big. This could be due to the fact that preheating temperatures are not high enough to cause major, and significant microstructural alteration.

The following are valid for Figure 4.3 and Figure 4.4.

1. For the Inco 182 welded samples:
   - % Elongation Equation is: %El = - 0.0145 (T) + 35.369, with $R^2 = 0.9565$ where preheat temperture T is measured in °F.
   - % Reduction of Cross Sectional Area Equation is: %RA = - 0.0096 (T) + 82.211, with $R^2 = 0.6113$

2. For the E309 welded samples:

   - % Elongation Equation is: %El = - 0.0082 (T) + 34.379, with $R^2 = 0.5698$

   - % Reduction of Cross Sectional Area Equation is: %RA = - 0.0152 (T) + 80.533, with $R^2 = 0.783$.

Table 4.2. Percentage elongation and reduction in cross sectional area @ different preheat temp.

Weld Metal	Welding Condition	% Elongation	% Reduction of Area
Inco 182	No Preheat	35.3	81.78
	350°F Preheat	30	80.64
	350°F Preheat	32	79.93
	400°F Preheat	29	78.84
	400°F Preheat	28.5	79.93
	450°F Preheat	28	74.8
	450°F Preheat	30	76.96
E-309	No Preheat	34.8	80.6
	350°F Preheat	31.9	74.6
	350°F Preheat	28	72.96
	400°F Preheat	31.5	78.84
	400°F Preheat	29.3	74.6
	450°F Preheat	33.5	76.96
	450°F Preheat	31.5	68.64

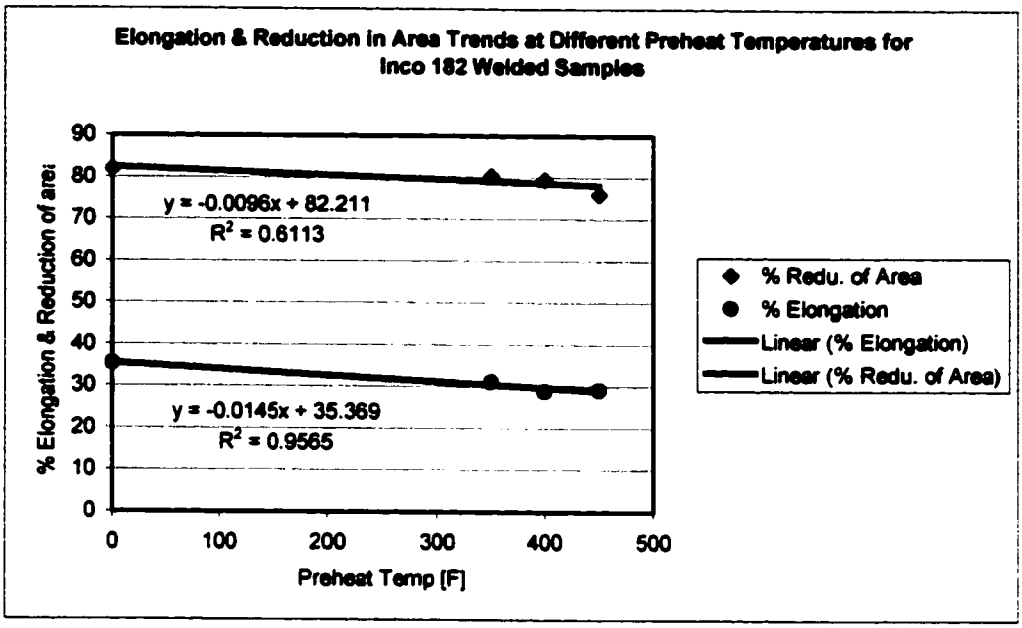

Figure 4.3 Graph representation for the percentage elongation & reduction in area at different preheat temperature for Inco 182 welded samples.

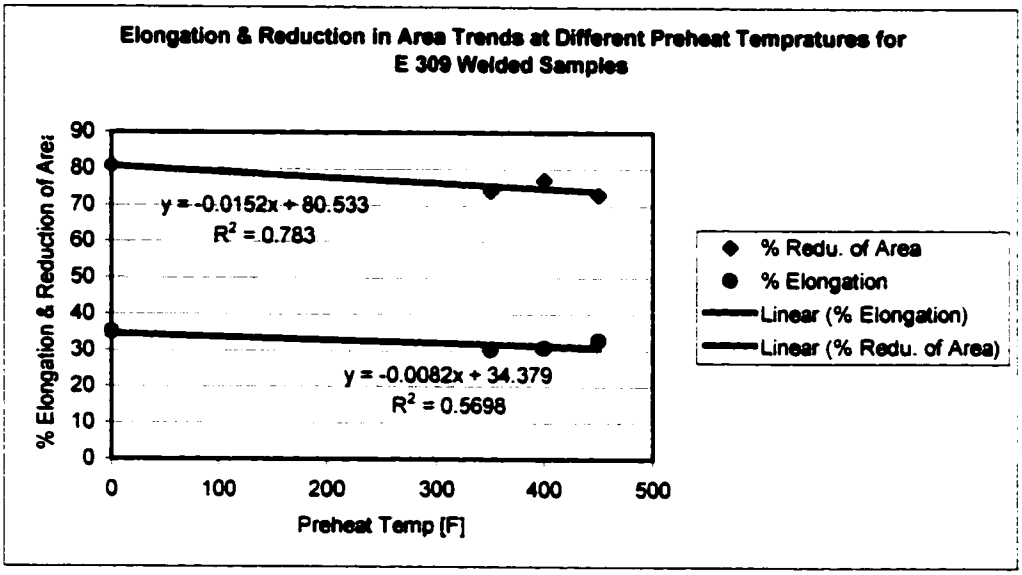

Figure 4.4. Graph representation for the percentage elongation & reduction in area at different preheat temperature for E 309 welded samples.

4.2 Metallographic Examination Prior To NACE Testing

Metallographic examination conducted on samples sectioned from all welded plates (3 samples X 8 plates) showed different degree of hard zones formation. This can be observed in the Figures 4.6 to 4.10.

As can be seen from the following set of photo-micrographs, the problem area of DMWs is the fusion line region on the carbon steel side of the joint. This is because of the existence of very thin, non-continuous layers of hard zones along the fusion line. The hard zones (or intermediate mixed zones) are very thin, noncontinuous layers, typically 0.025 mm (0.001 in) wide, with a hard microstructure. They are of intermediate composition between the carbon steel base metal and the bulk weld metal composition.

Doody [1] conducted Energy Dispersive X-Ray Spectrometry (EDS) on several different DMWs prepared using different welding electrodes (E 309, and Inco 182 were included). EDS results showed that the hard zones have low alloy compositions, typically 3-5% chromium and 2-3% nickel. Doody reported that, microhardness and microprobe (Electron Probe X-Ray Microanalysis, EPMA) analysis in many other investigations have consistently confirmed the low alloy composition and high hardness of the hard zones.

Figure 4.5 is a schematic diagram of a DMW cross-section and a magnified view of the hard zone at the fusion line along the carbon steel side of the joint. The intermediate mixed zone is about 30 microns in width. This zone, as stated earlier has low alloy compostion.

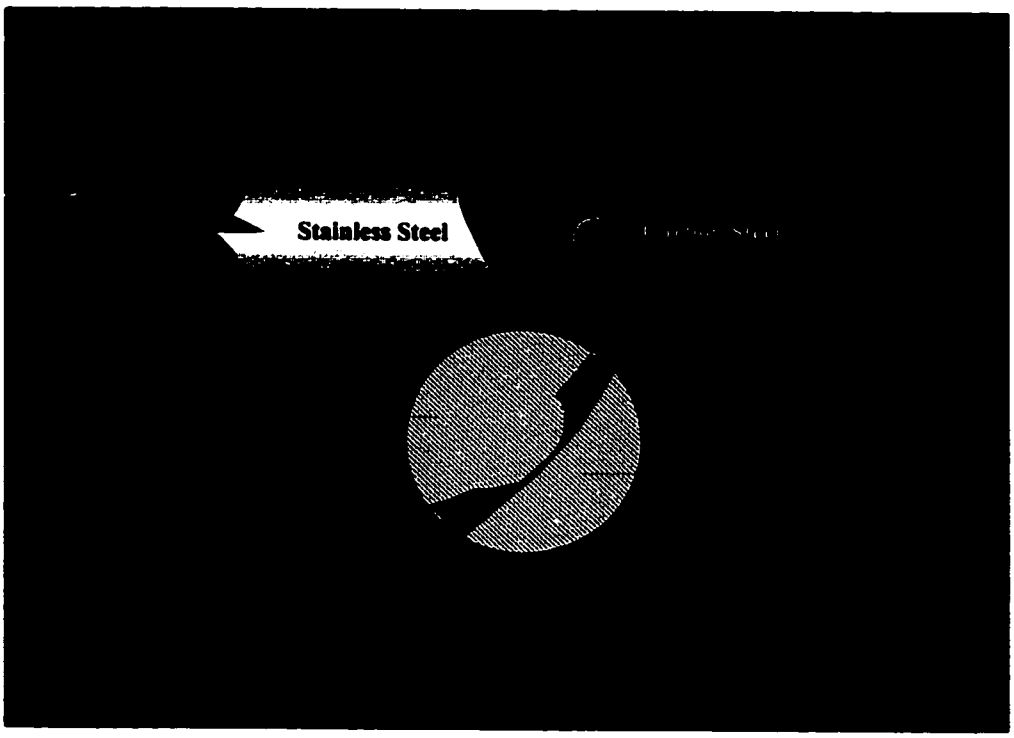

Figure 4.5. Schematic diagram of a DMW cross-section and a magnified view of the hard zone at the fusion line along the carbon steel side of the joint

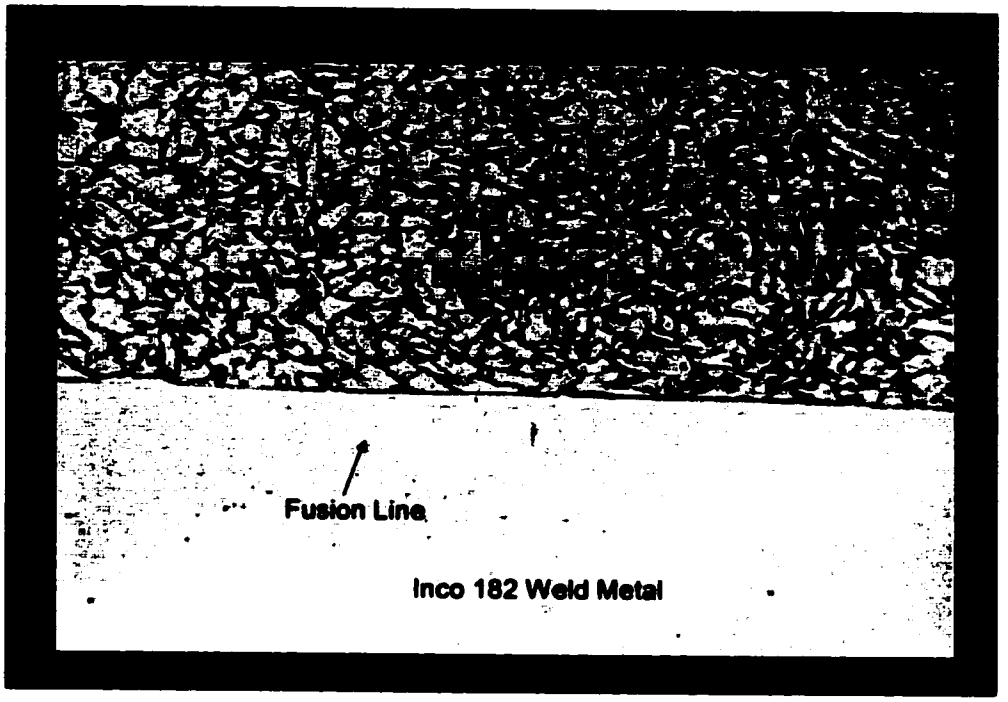

Figure 4.6. Clear fusion line between the C.S base metal (top), and Inco 182 filler electrode. Welded @ 400°F preheat, 400X.

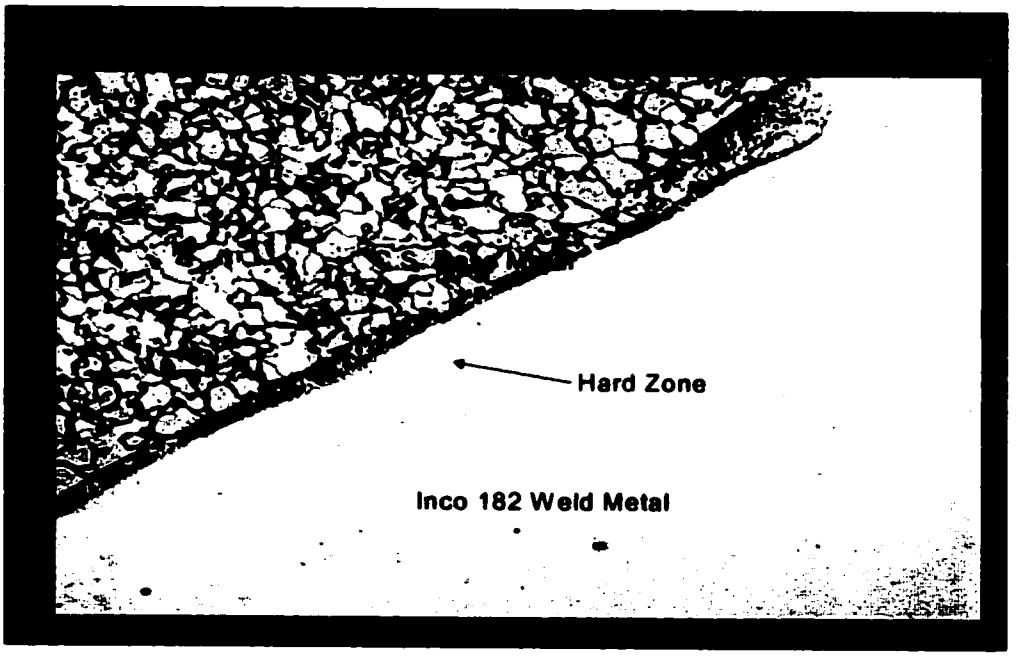

Figure 4.7. Hard zone formed at the fusion line between the C.S. (Top Left) and the Inco 182 filler. Welded @ 450°F preheat condition, 200X.

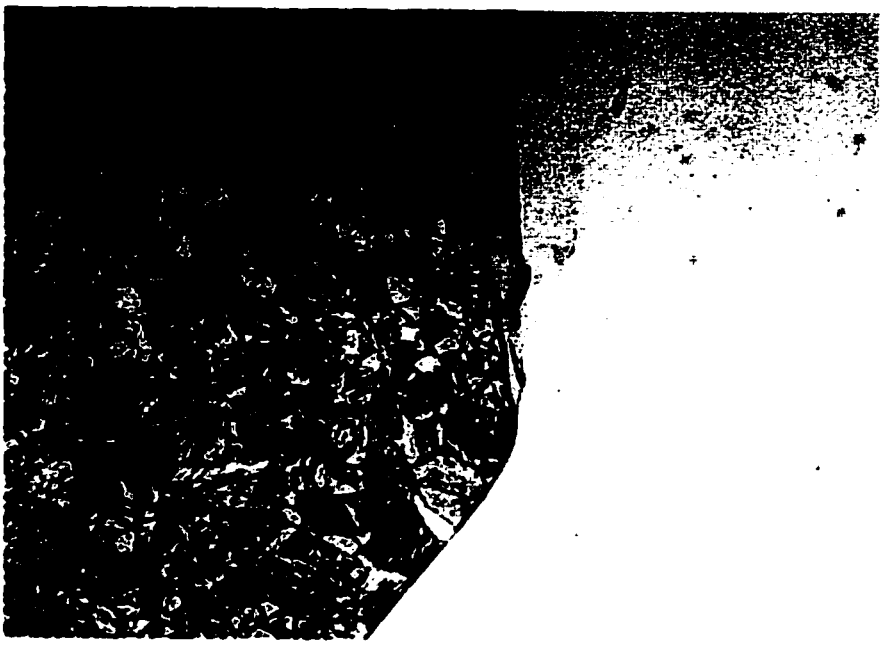

Figure 4.8. Hard zone (top and center of the fusion line) formed between the C.S. base metal (left) and Inco 182, while the bottom part of the fusion line is clear, and distenict. Welded @ 350°F preheat, 100X.

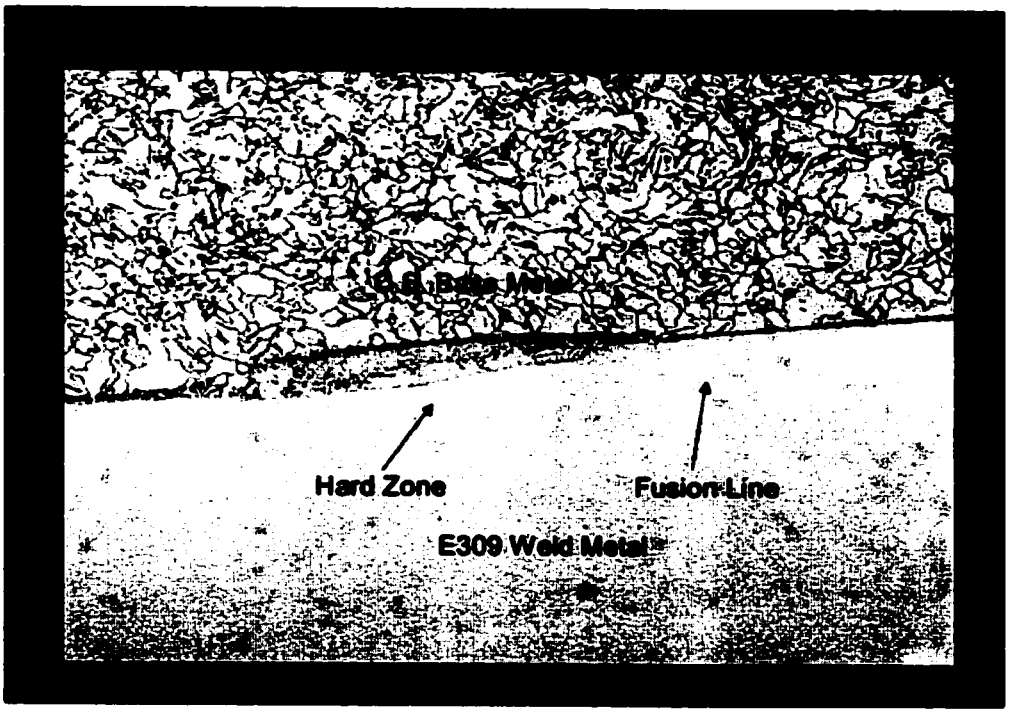

Figure 4.9. Hard zone at the center of the fusion line beween the C.S. base metal (top), and E 309 filler. Welded @ 400°F preheat condition, 200X.

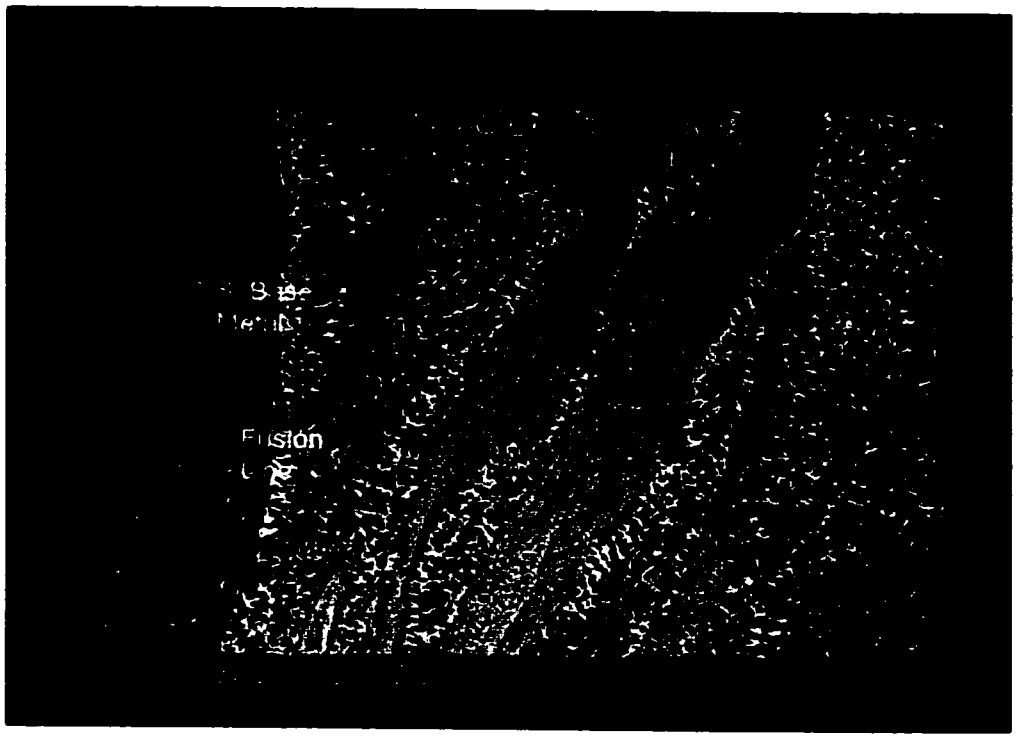

Figure 4.10. Hard zone formed within the bulk weld metal (center of the photograph, white section), E 309 welded sample @ 350°F, 100X.

Two explanations for the formation of hard zones exist in the literature:

1) Based on the EDS and microstructural analysis, it was found that the microstructures of these zones consist of chromium carbides in a martensite matrix. This suggest that diffusion of strong carbide formers (e.g. Cr, W) from the filler metal and carbon from the base metal create a region along the fusion line rich in chromium and tungsten carbides with a martensitic structure [12]. Even though the time at elevated temperatures during the welding cycles is short, some slight carbon depletion of carbon steel HAZ has occasionally been observed [1]. This indicates that there is some carbon diffusion into the weld metal and the hard zones.

2) As the mechanical hydrodynamic mixing of the molten boundary into the weld metal does not occur, it is believed that these hard zones are unmixed chunks of carbon steel that were not diluted in the bulk weld metal. This is why its actual composition intermediate between the base metal and the diluted bulk weld metal.

EDS and microhardness surveys were conducted on selective sample to confirm the chemical composition and microhardness of the hard zones, and the area around them. Findings of these surveys are summarized in Table 4.3. Details of the EDS analysis are in the appendix.

Table 4.3. EDS and microhardness surveys results.

Position	Inco 182 Welded Samples		E 309 Welded Samples	
	Micro-Hardness [VHN]	Chemical Comp. [wt%]	Micro-Hardness [VHN]	Chemical Comp. [wt%]
Weld Metal	183	7.09 Cr; 3.06 Mn; 59.98 Fe; 29.56 Ni	211	8.97 Cr; 1.46 Mn; 83.15 Fe; 5.58 Ni
Before H.Z.	97.3		191	
@ H. Z.	323		405	
After H.Z.	182		203	
Base Metal	186		191	

From the two above explanations on the formation of the hard zones, and based on the results and findings obtained from the metallographical examination, and the EDS survey, it is apparent that filler metals with any appreciable chromium content will produce a similar hard zone in the fusion line as presented.

These findings explain why E 309 (Austenitic with 24 wt% Cr) was producing welds with very high amount of hard zone, and hence high susceptibility to SSC (as will be seen later) compare to Inco 182 (Ni-base with 15 wt %Cr).

Moreover, this study has indicated that the hard zones are still present even with the nickel-based electrodes, but that the size and frequency might be reduced, in comparison to the austenitic stainless steel electrodes. However, it does not appear that the hard zones can be reliably eliminated for manual welding methods, even with the nickel-base electrode, and the optimum preheat temperature.

4.3 NACE Standard Tensile Test

Time-To-Failure (TTF) results of specimens are shown in Table 4.4 and 4.5 for the Inco 182, and E309 welds, respectively. Initial and final pH of the test solution is also shown.

To simplify the data, the average time-to-failure values and percentage of samples failed and samples passed the test are recorded in Table 4.6 and ploted in Figures 4.11 and 4.12.

Table 4.4. SSC test results for the Inco 182 Welds

Sample ID	Welding Condition	Level of Stress as % Y.S.	Applied Stress [ksi]	Initial pH	Final pH	TTF [HRs]
1AI	Inco 182, No P.H.	110	57.343	2.7	2.9	1.6
1AI	Inco 182, No P.H.	110	57.343	2.7	2.9	2.7
1AII	Inco 182, No P.H.	80	41.704	2.7	3.2	14
1AII	Inco 182, No P.H.	80	41.704	2.7	3.2	17.9
1AIII	Inco 182, No P.H.	60	31.278	2.7	3.72	720♦
1AIII	Inco 182, No P.H.	60	31.278	2.7	3.75	720♦
1BI	Inco 182, 350°F P.H.	110	53.724	2.6	3.2	1
1BI	Inco 182, 350°F P.H.	110	53.724	2.6	3.4	1
1BII	Inco 182, 350°F P.H.	80	39.072	2.8	3.2	13.7
1BII	Inco 182, 350°F P.H.	80	39.072	2.8	3.4	4.5
1BIII	Inco 182, 350°F P.H.	60	29.304	2.7	3.5	148.3
1BIII	Inco 182, 350°F P.H.	60	29.304	2.7	3.5	126.3
1CI	Inco 182, 400°F P.H.	110	61.402	2.6	3.2	3.7
1CI	Inco 182, 400°F P.H.	110	61.402	2.6	3.1	4.9
1CII	Inco 182, 400°F P.H.	80	44.656	2.5	3.45	83.1
1CII	Inco 182, 400°F P.H.	80	44.656	2.5	3.43	137.3
1CIII	Inco 182, 400°F P.H.	60	33.492	2.5	3.85	720♦
1CIII	Inco 182, 400°F P.H.	60	33.492	2.5	3.61	226
1DI	Inco 182, 450°F P.H.	110	53.394	2.6	3.1	0.95
1DI	Inco 182, 450°F P.H.	110	53.394	2.6	3.1	0.9
1DII	Inco 182, 450°F P.H.	80	38.832	2.7	3.56	121.6
1DII	Inco 182, 450°F P.H.	80	38.832	2.7	3.2	49.8
1DIII	Inco 182, 450°F P.H.	60	29.124	2.7	3.6	174.5
1DIII	Inco 182, 450°F P.H.	60	29.124	2.7	3.75	259

Note: the numbering system followed for samples ID is as follows:
1= Inco 182 filler metal.
A = no preheat, B = 350 °F preheat, C = 400 °F preheat, D = 450 °F preheat.
I= Loaded at 110% Y.S, II= Loaded at 80% Y.S, III= Loaded at 60% Y.S.
♦ Specimen not failed at 720 hrs of exposure.

Table 4.5. SSC test results for the E309 welds.

Sample ID	Welding Condition	Level of Stress as % Y.S.	Applied Stress [ksi]	Initial pH	Final pH	TTF [HRs]
3AI	E-309, No P.H.	110	58.971	2.7	3.1	4.8
3AI	E-309, No P.H.	110	58.971	2.7	3.2	4
3AII	E-309, No P.H.	80	42.888	2.7	3.8	120.3
3AII	E-309, No P.H.	80	42.888	2.7	3.7	84.3
3AIII	E-309, No P.H.	60	32.166	2.7	3.7	262.1
3AIII	E-309, No P.H.	60	32.166	2.7	3.7	264.1
3BI	E-309, 350°F P.H.	110	62.183	2.7	3.37	0.7
3BI	E-309, 350°F P.H.	110	62.183	2.7	3.1	0.4
3BII	E-309, 350°F P.H.	80	45.224	2.7	3.35	5.6
3BII	E-309, 350°F P.H.	80	45.224	2.7	3.15	5.3
3BIII	E-309, 350°F P.H.	60	33.918	2.7	3.6	161.6
3BIII	E-309, 350°F P.H.	60	33.918	2.7	3.37	720♦
3CI	E-309, 400°F P.H.	110	57.365	2.6	2.9	1.4
3CI	E-309, 400°F P.H.	110	57.365	2.6	3.2	1.2
3CII	E-309, 400°F P.H.	80	41.72	2.5	3.08	3.6
3CII	E-309, 400°F P.H.	80	41.72	2.5	2.8	3.7
3CIII	E-309, 400°F P.H.	60	31.29	2.5	2.95	1.2
3CIII	E-309, 400°F P.H.	60	31.29	2.5	3.1	1.5
3DI	E-309, 450°F P.H.	110	52.8	2.6	3.56	106
3DI	E-309, 450°F P.H.	110	52.8	2.6	3.55	106
3DII	E-309, 450°F P.H.	80	38.4	2.7	3.6	166.5
3DII	E-309, 450°F P.H.	80	38.4	2.7	3.05	7.9
3DIII	E-309, 450°F P.H.	60	28.8	2.7	3.68	236.2
3DIII	E-309, 450°F P.H.	60	28.8	2.7	3.7	236

Note: the numbering system followed for samples ID is as follows:
3= E-309 filler metal.
A= no preheat, B= 350 °F preheat, C= 400 °F preheat, D= 450 °F preheat.
I= Loaded at 110% Y.S, II= Loaded at 80% Y.S, III= Loaded at 60% Y.S.
♦ Specimen not failed at 720 hrs of exposure.

Table 4.6. Avg. TTF with percentage of samples that failed or passed the SSC test.

Filler	Welding Condition	Level of Stress as % Y.S.	Average Applied Stress Value [ksi]	Average TTF [HRs]	% Samples Failed	% Samples Passed
Inco 182	No Pre-heat	110	57.343	2.15	100%	0%
	No Pre-heat	80	41.704	15.95	100%	0%
	No Pre-heat	60	31.278	720	0%	100%
Inco 182	350°F Pre-heat	110	53.724	1	100%	0%
	350°F Pre-heat	80	39.072	9.1	100%	0%
	350°F Pre-heat	60	29.304	137.3	100%	0%
Inco 182	400°F Pre-heat	110	61.402	4.3	100%	0%
	400°F Pre-heat	80	44.656	110.2	100%	0%
	400°F Pre-heat	60	33.492	473	50%	50%
Inco 182	450°F Pre-heat	110	53.394	0.925	100%	0%
	450°F Pre-heat	80	38.832	85.7	100%	0%
	450°F Pre-heat	60	29.124	216.75	100%	0%
E309	No Pre-heat	110	58.971	4.4	100%	0%
	No Pre-heat	80	42.888	102.3	100%	0%
	No Pre-heat	60	32.166	263.1	100%	0%
E309	350°F Pre-heat	110	62.183	0.55	100%	0%
	350°F Pre-heat	80	45.224	5.45	100%	0%
	350°F Pre-heat	60	33.918	440.8	50%	50%
E309	400°F Pre-heat	110	57.365	1.3	100%	0%
	400°F Pre-heat	80	41.72	3.65	100%	0%
	400°F Pre-heat	60	31.29	1.35	100%	0%
E309	450°F Pre-heat	110	52.8	106	100%	0%
	450°F Pre-heat	80	38.4	87.2	100%	0%
	450°F Pre-heat	60	28.8	236.1	100%	0%

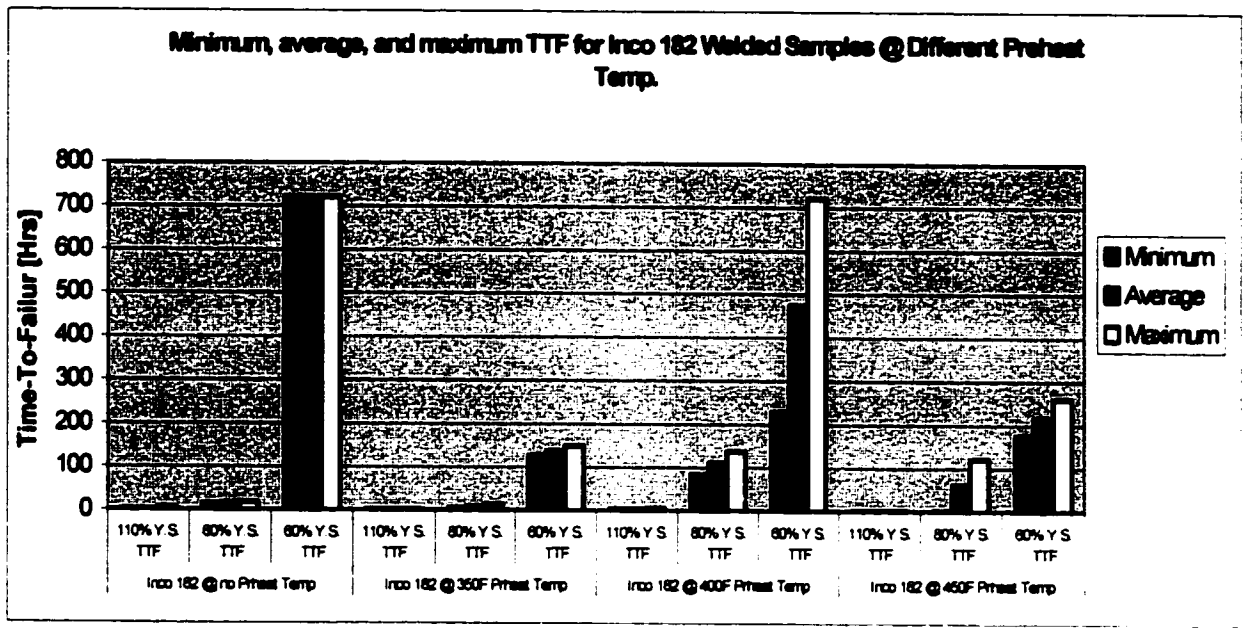

Figure 4.11. Min., avg., and max. TTF for Inco 182 at different preheat temperature.

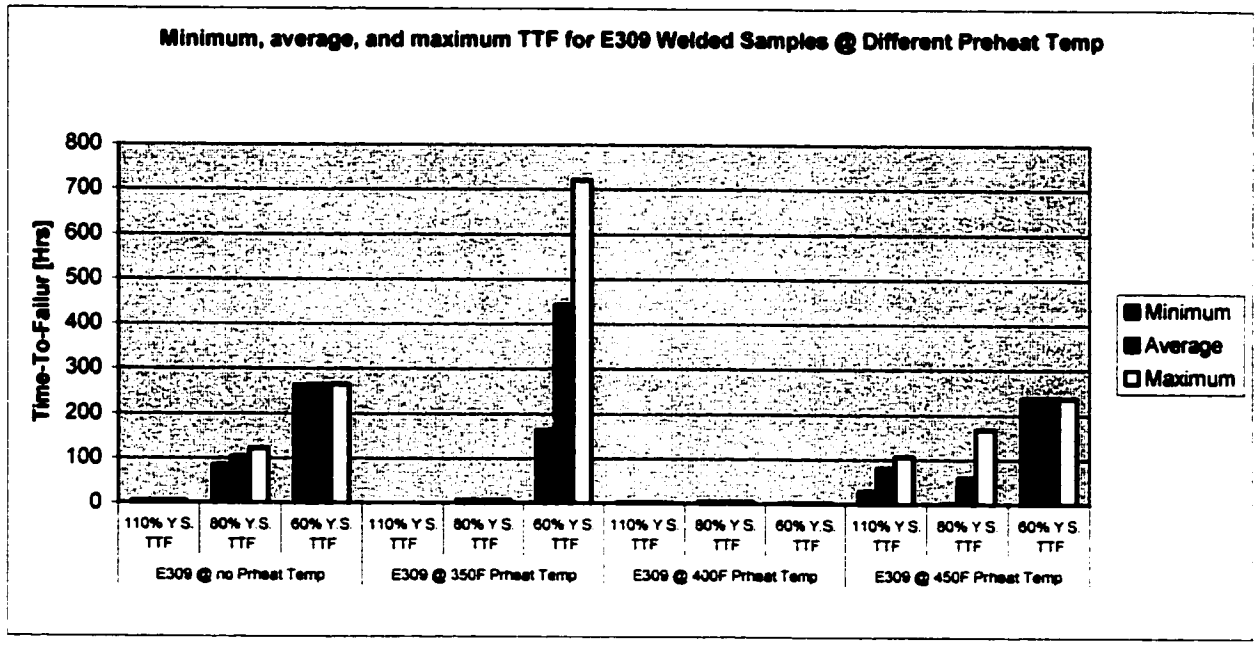

Figure 4.12. Min., avg., and max. TTF for E 309 at different preheat temperture.

With reference to NACE standard TM 01-77-96, and based on the results presented in Tables 4.4 and 4.5 (Time-To-Failure), it can be said that both Inco 182 and E-309 electrodes produce welds with very high susceptibility to sulfide stress cracking. Nonetheless, there has been considerable improvement in the TTF for the Inco 182 welded samples at 400°F (205°C) as can be noticed in Figures 4.13 and 4.14 where the relation between TTF and the preheat temperatures are presented.

These results support the results reported by Omar [9-10], as the 400°F (205°C) is the optimum preheat temperature for the Inco 182 electrode in welding DMWs. It is the 400°F (205°C) preheat temperature that result in an optimum cooling rate that help in avoiding the formation of the martensitic zones during the solidification process of the weld and base metals.

According to Omar, the optimum preheat temperature lies in a very narrow range of about 50°F (28°C), above or below which the hard zone formation increases. This explains why the 350°F (177°C) and 450°F (232°C) preheating temperatures have produced welds with relatively high susceptibility to SSC (low TTF).

Multiple metallographic cross-sections of all test plates confirmed the above findings as it can be noticed in the set of photo-microstructures presented in section 4.2.

On the other hand as indicated in Figure 4.14, no consistent relation could be found between the preheating temperatures and the average time to failure for the E 309 welded samples. It can be noticed, from Figure 4.13 and Figure 4.14, that the TTF improves as the %Y.S. loading decreases. This is true for both type of welded samples regardless the preheating temperature.

The time-to failure versus the applied stress representation as shown in NACE TM 01-77-96 is presented in Figures 4.15-a, b, c, d, and Figures 4.16-a, b, c, d for each welding condition. The estimated threshold stress value, which is the maximum stress the material can sustain without failure for 720 hrs or more, for the different welding conditions are summarized in Table 4.7. The equivalent %Y.S. value for each estimated threshold stress is also given. Most of these values are below the standard design criteria used within Saudi Aramco (between 60 to 80 %Y.S.) and much below the acceptance criteria of 90% of the Y.S. published by the European Federation of Corrosion (EFC) and listed in their publication No 16 for welded piping, pipeline, and pressure vessels that are 90% of the Y. S. [21].

Based on the results obtained from the SSC test and considring TTF as the measuring factor, ranking of the preheat tempertures in terms of their postive effect on the TTF can be done by utilizing Figures 4.17.

In the case of Inco 182 welded samples, the following observations may be made:

- The 400°F preheat temperture resulted in longest TTF at all leveles of applied stresses.
- At stress level between 35 and 55 ksi, 350°F and 450°F preheat result in the same time to failure.
- The 450°F preheat temperture was the 2nd best in term of its positive effect on TTF at all applied stress levels.
- And finally, the 350°F preheat temeprture was the worst in term of TTF.

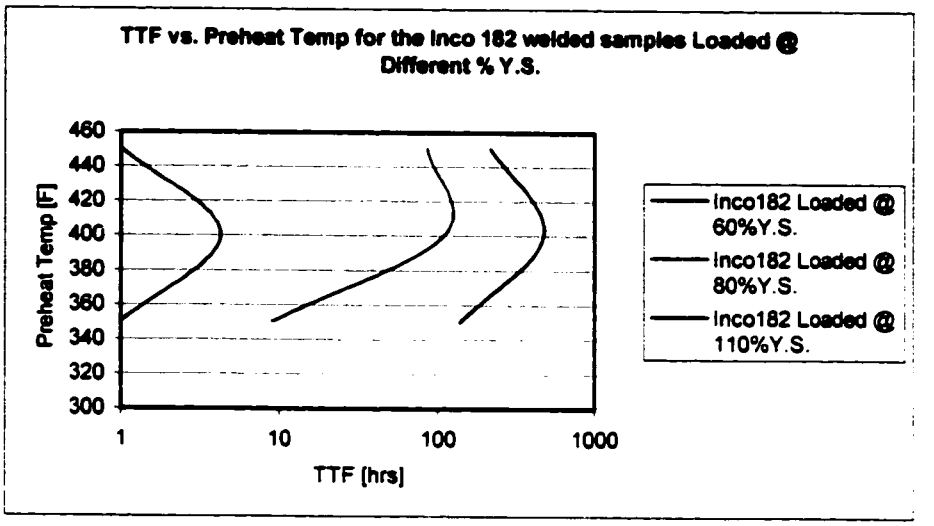

Figure 4.13. Improvement in the TTF @ 400°F for the Inco 182 welded samples.

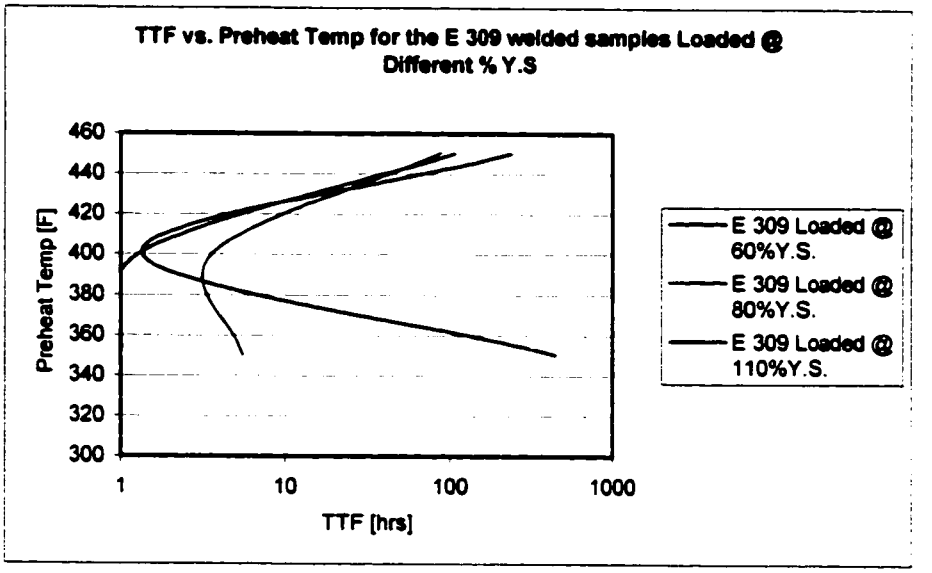

Figure 4.14. TTF trend for E 309 welded samples.

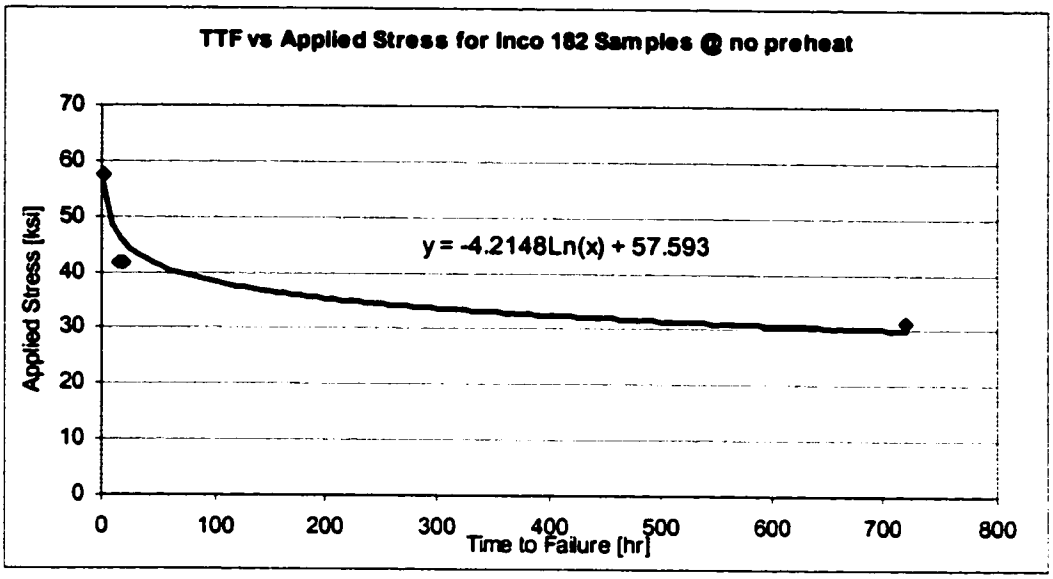

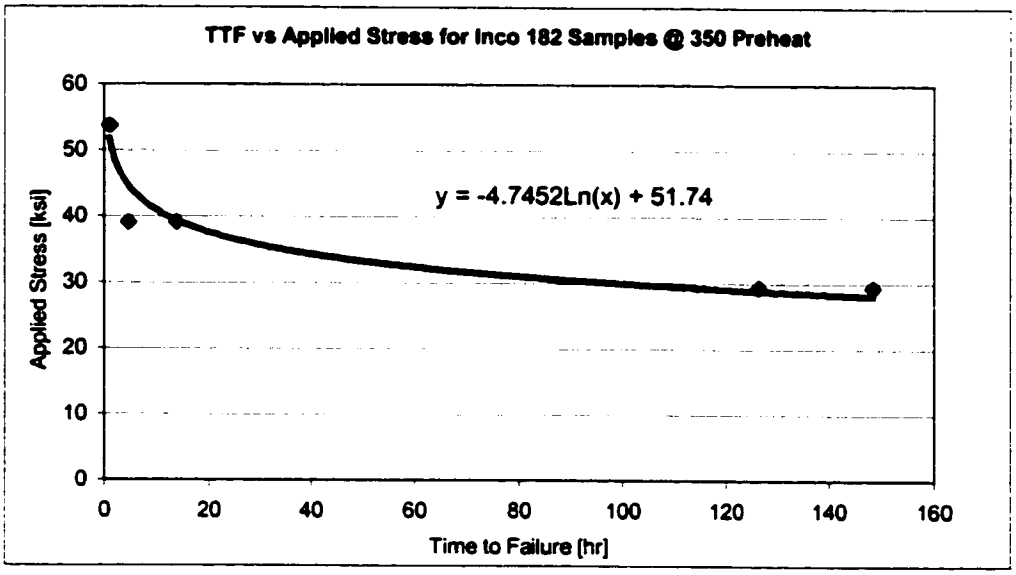

Figures 4-15 a&b. TTF vs Applied stress representation as presented in NACE TM01-77, where y = Applied stress (ksi), and x = Time to failure in hours

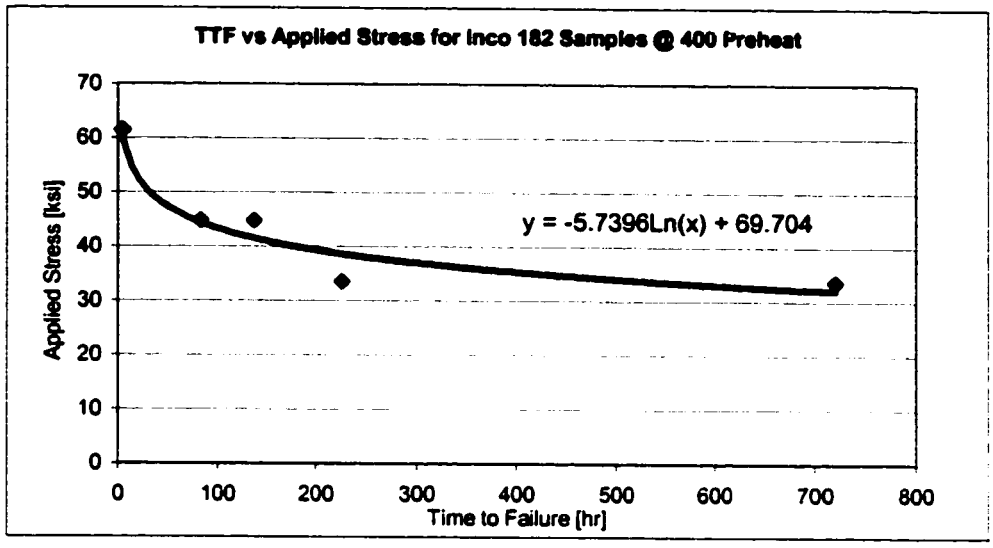

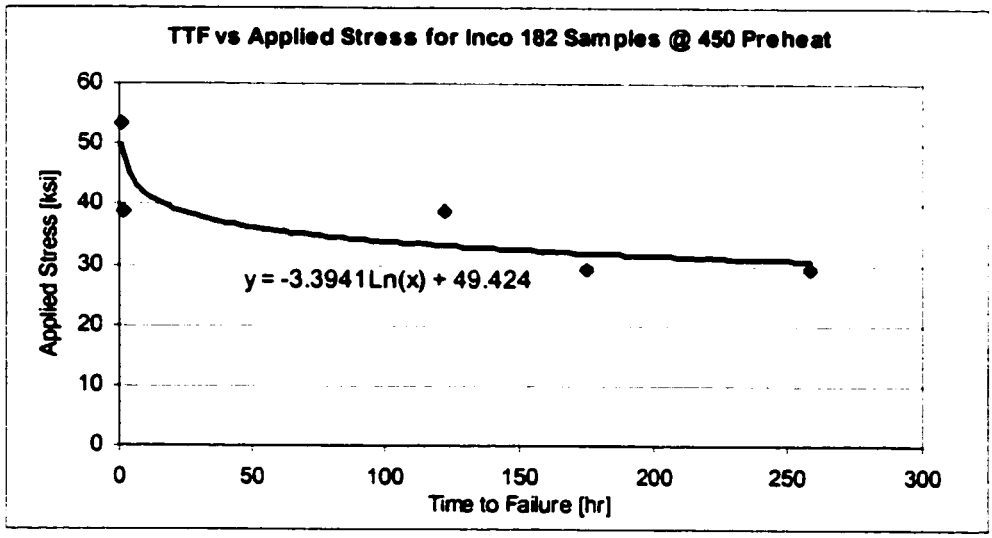

Figures 4.15 c&d. TTF vs Applied stress representation as presented in NACE TM01-77, where y = Applied stress (ksi), and x = Time to failure in Hours.

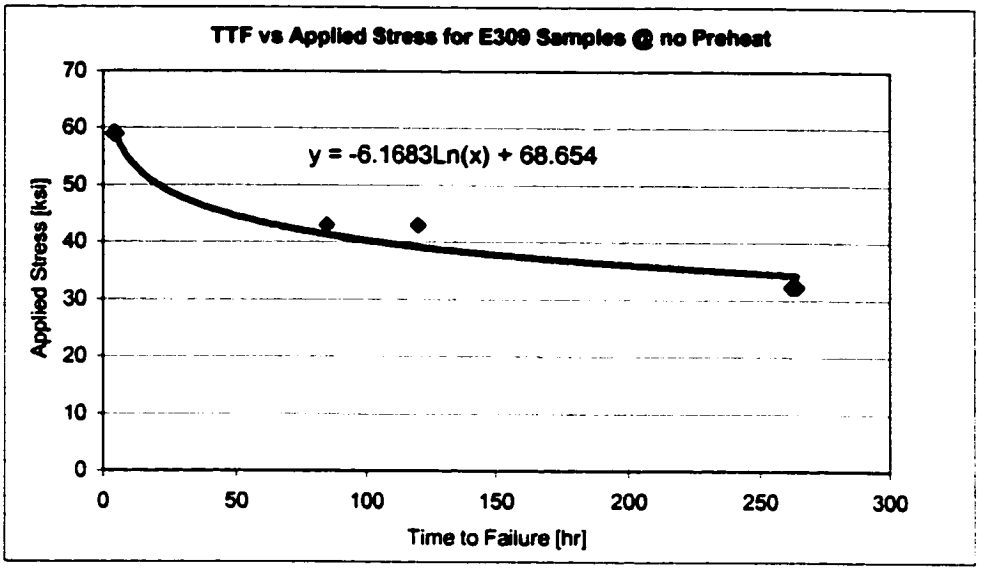

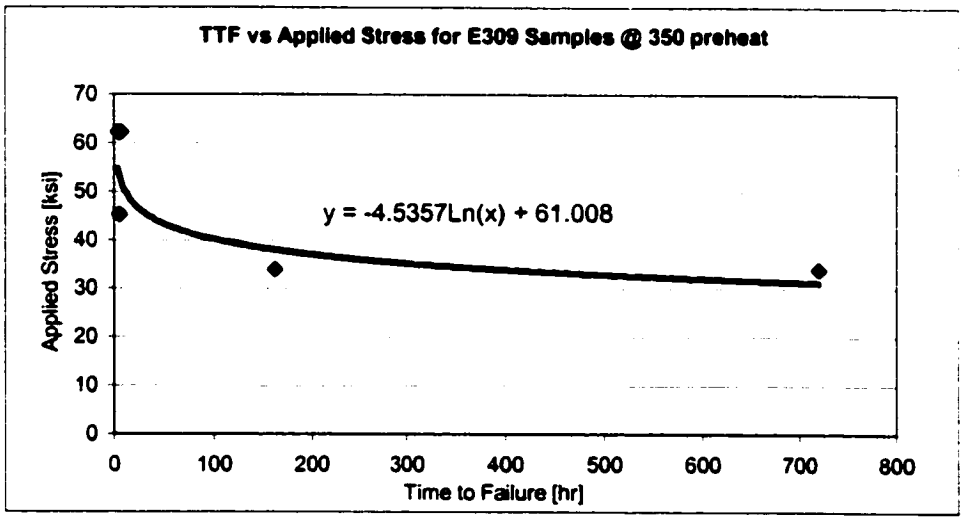

Figures 4.16 a&b. TTF vs Applied stress representation as presented in NACE TM0177, where y = Applied stress (ksi), and x = Time to failure in hours.

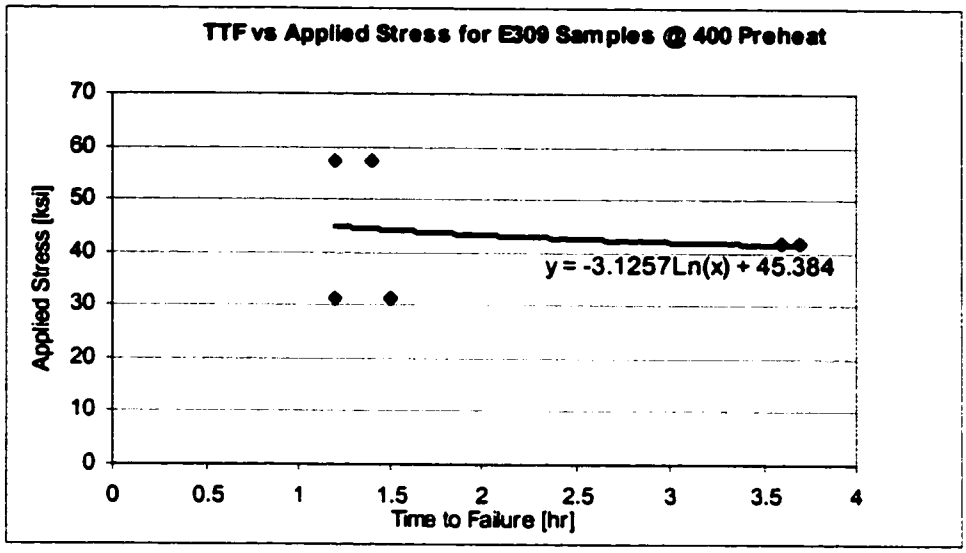

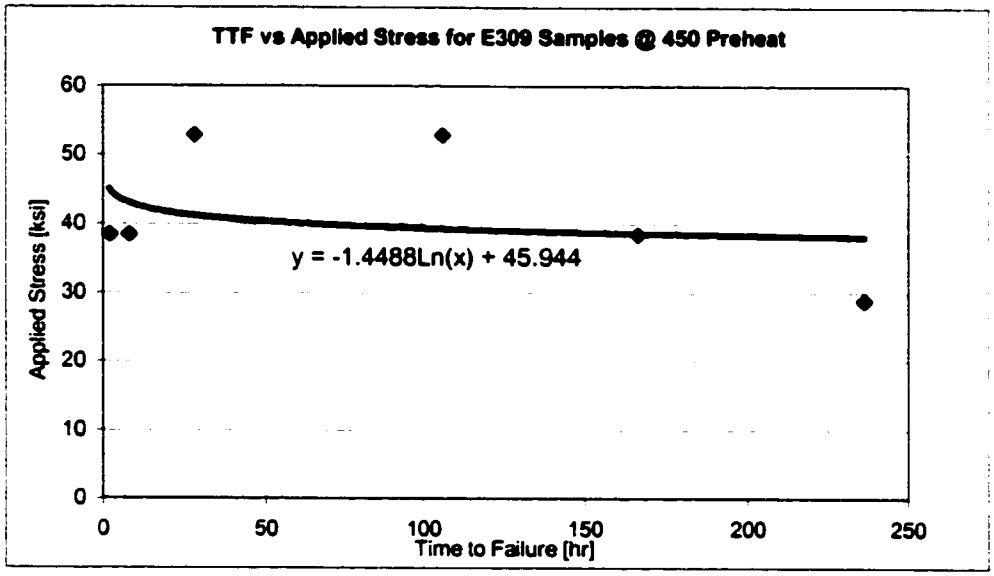

Figures 4.16 c&d. TTF vs Applied stress representation as presented in NACE TM0177, where y = Applied stress (ksi), and x = Time to failure in Hours.

Table 4.7. Estimated threshold stress values in H_2S environment.

Weld Metal	Welding Condition	Estimated Threshold Stress [Ksi]	Average Y.S. [Ksi]	Approximate %YS for the Threshold Stress
Inco 182	No Pre-heat	30	52.13	57.5% of the Y.S.
	350°F Pre-heat	28	48.84	57.3% of the Y.S.
	400°F Pre-heat	33	55.82	59.1% of the Y.S.
	450°F Pre-heat	30	48.535	61.8% of the Y.S.
E-309	No Pre-heat	35	53.61	65.3% of the Y.S.
	350°F Pre-heat	32	56.525	56.6% of the Y.S.
	400°F Pre-heat	41	52.145	78.6% of the Y.S.
	450°F Pre-heat	38	48	81.3% of the Y.S.

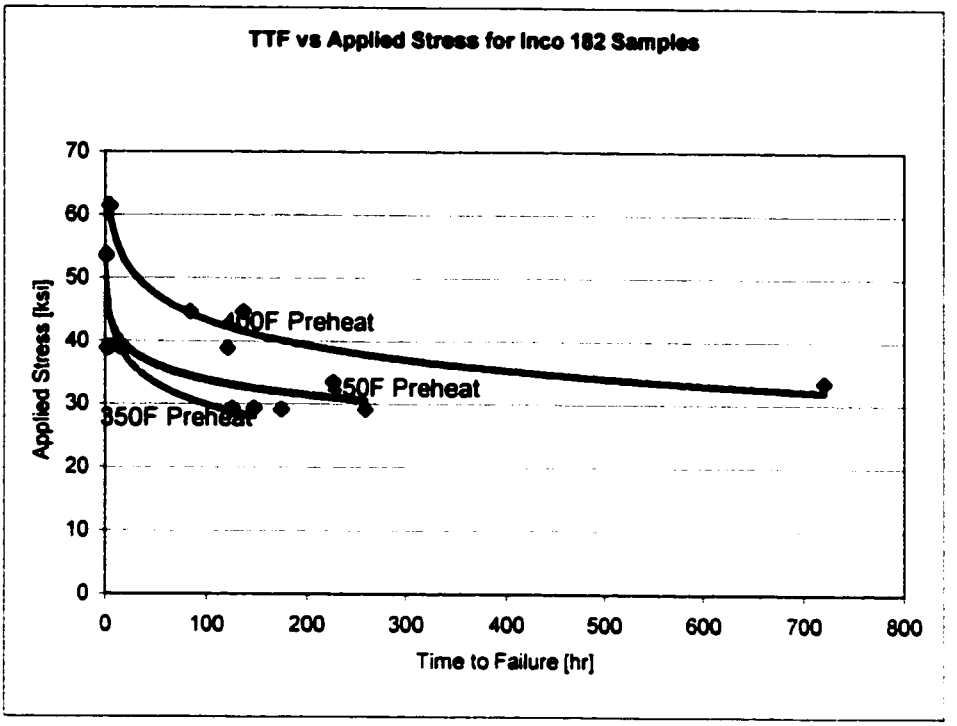

Figure 4.17. Ranking of preheat tempetures based on TTF.

4.4 Metallographic and Scanning Electron Examination After SSC Test

Figures 4.18-a and b are photo-micrographs for typical samples that passed the NACE SSC Proof Ring test and those that failed the test. In figure 4.18-b, it is clearly that the fracture is along the weld fusion interface with the carbon steel base metal. Visually, most of the failures were brittle failures along the weld fusion interface with the carbon steel base metal.

Figure 4.19 is a cross section through the gauge length of a failed sample (carbon steel side at the top, and the stainless steel side with the weld metal at the bottom).

Cracks initiate at the hard zones and go along the fusion line between the carbon steel and the weld metal. The crack may propagate into the carbon steel HAZ. This can be noticed as follows:

- Figure 4.20, the carbon steel side of a failed sample showing traces of a white band (hard zone) attached to the carbon steel base metal.
- Figure 4.21, the stainless steel side of the same sample shown in Figure 4.20 where part of the carbon steel HAZ has detached with the bulk weld metal confirming the propagation of the crack as indicated above.

Figures 4.18-a. Photograph of samples passed the SSC test.

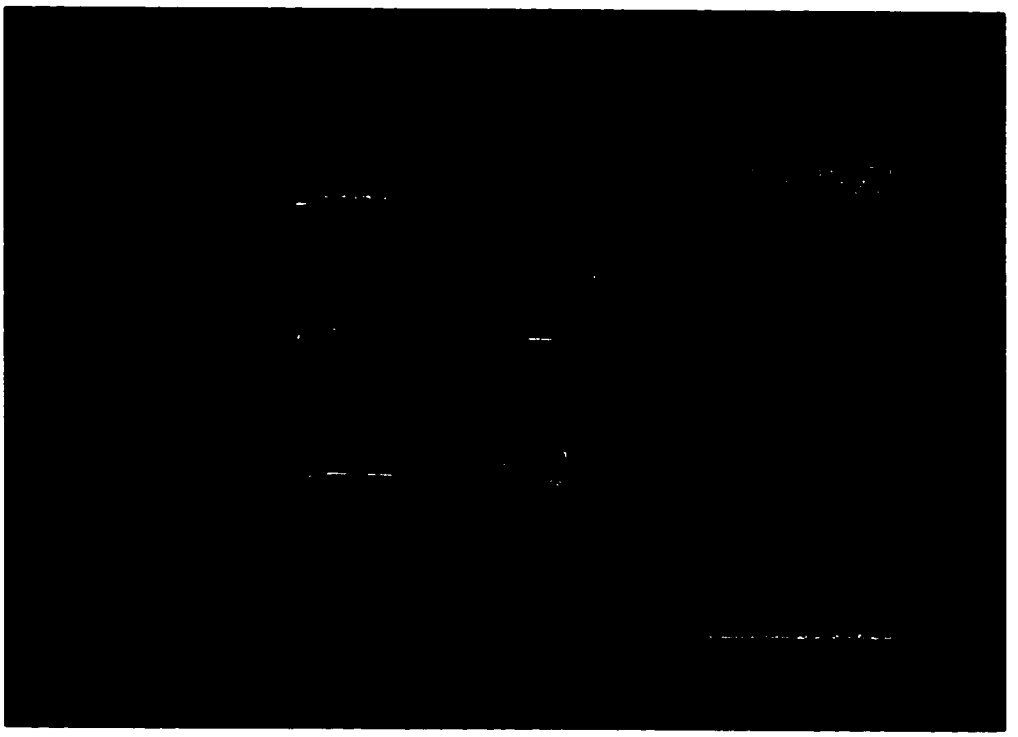

Figures 4.18-b. Photograph of samples failed the SSC test.

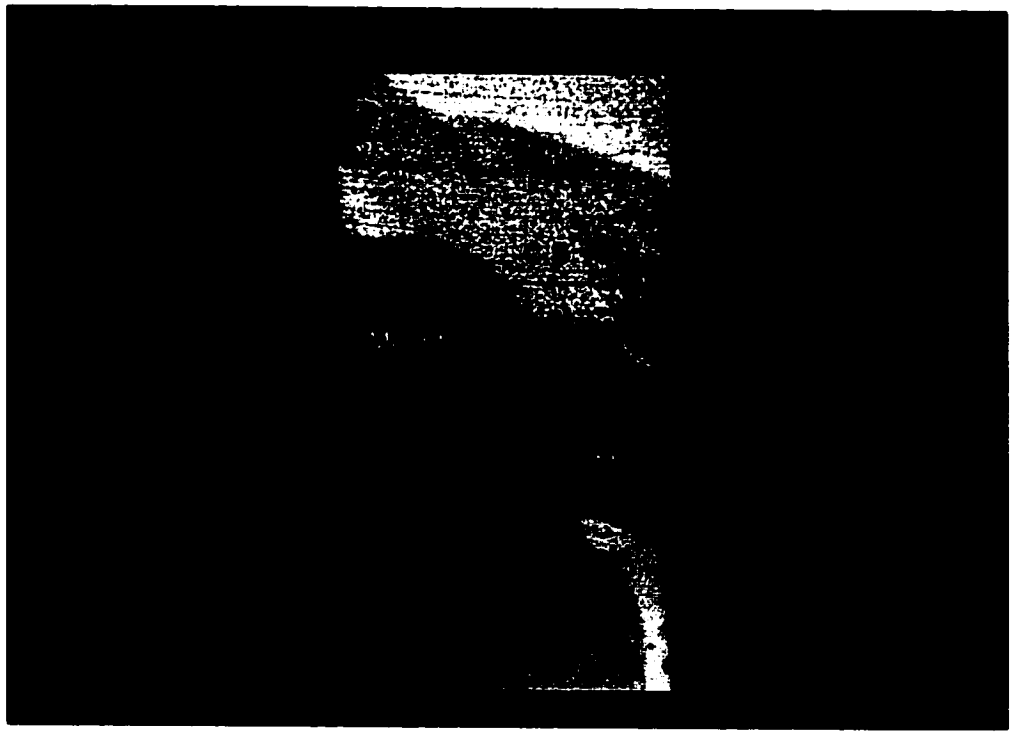

Figure 4.19. Cross section of a failed sample welded by Inco 182 @ 350°F preheat, (C.S side @ top, and S.S. + weld metal @ the bottom), 16X.

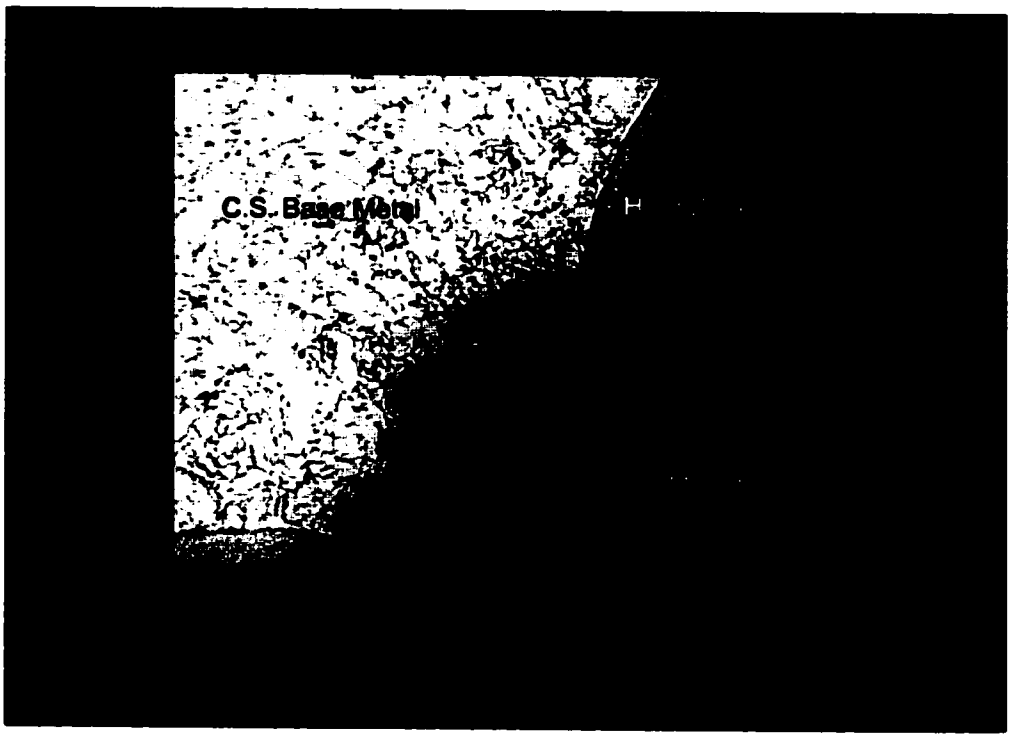

Figure 4.20. Carbon steel side of a failed sample welded with Inco 182 @ 350F preheat indicating crack path, 200X.

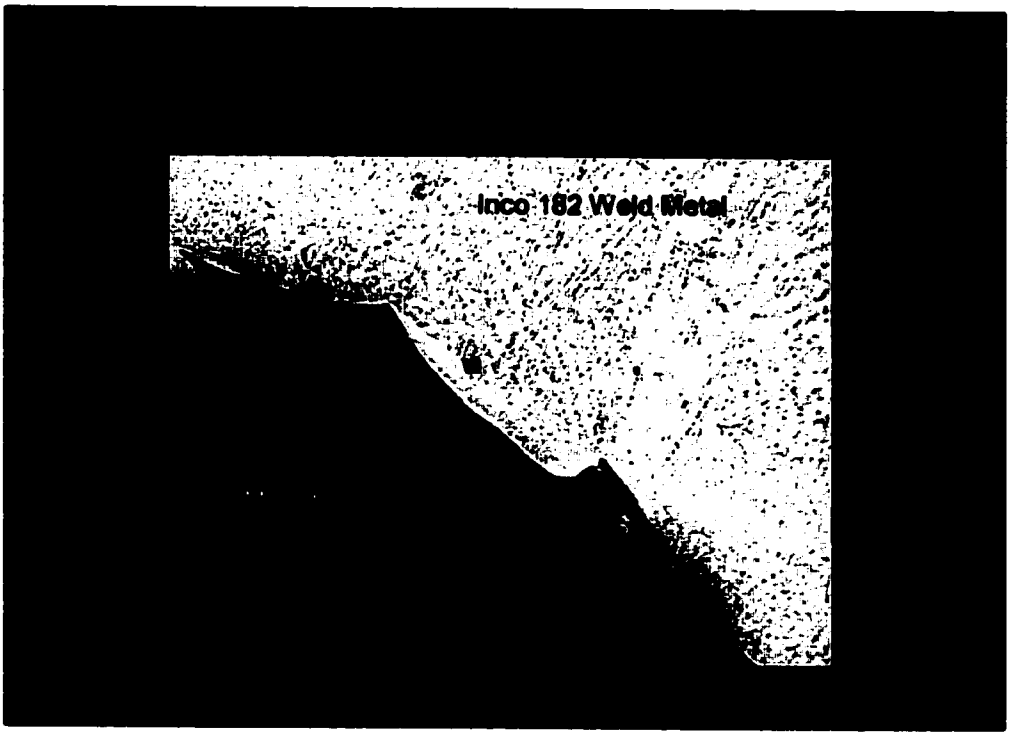

Figure 4.21. The stainless steel side of the same sample shown in figure 4.20, 63X.

Figures 4.22 throgh 4.29 show the fractography of selected surfaces (under the SEM) as they appeared after the NACE SSC Proof Ring Test.

Figure 4.22 is a low maginfication SEM of fracture surface of weld intrface, weld side, of an Inco 182 welded smaple with no preheat. From the surface profile two distinct fracture modes (Brittel and Ductile) can be observed.

Figure 4.23 is a higher magnification of the brittle section form Figure 4.22, area (A). This is a typical view observed in almost all the fracture surfaces. The weld metal solidification grain boundaries are clearly visible in the photograph.

Figure 4.24 is also a high magnification of another brittle region (area B in Figure 4.22). It shows similar features as in Figure 4.23.

Figure 4.25 is a high magnification of the ductile region of Figure 4.22 (area C) where a typical micro void coalescence fracture mode representing a ductile failure. This type of fracture was also noticed in almost all the fracture surfaces.

Figures 4.26 through 4.29 are set of fractographs from a sample welded using Inco 182 @ 400°F preheat temperature. Similar failure features were observed as in the previous set.

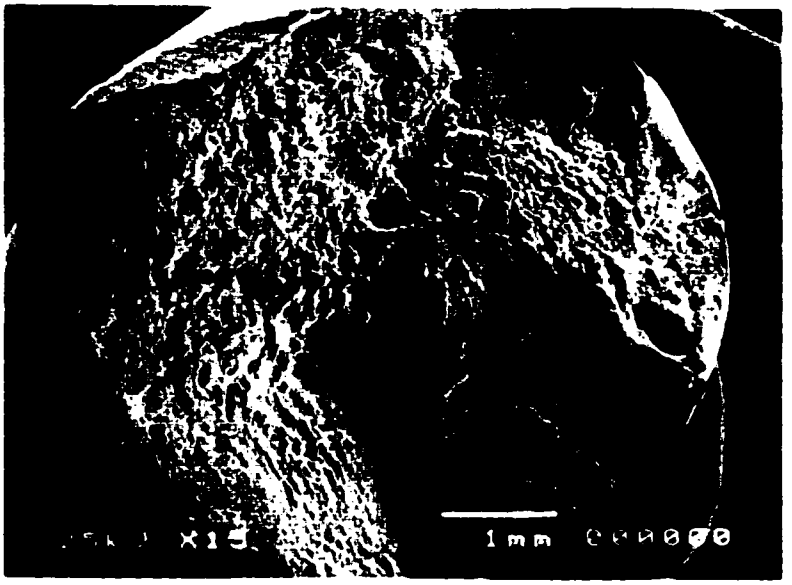

Figure 4.22. Low magnification SEM photograph of a fracture surface (S.S. Side) welded with Inco 182 @ no preheat, 15X.

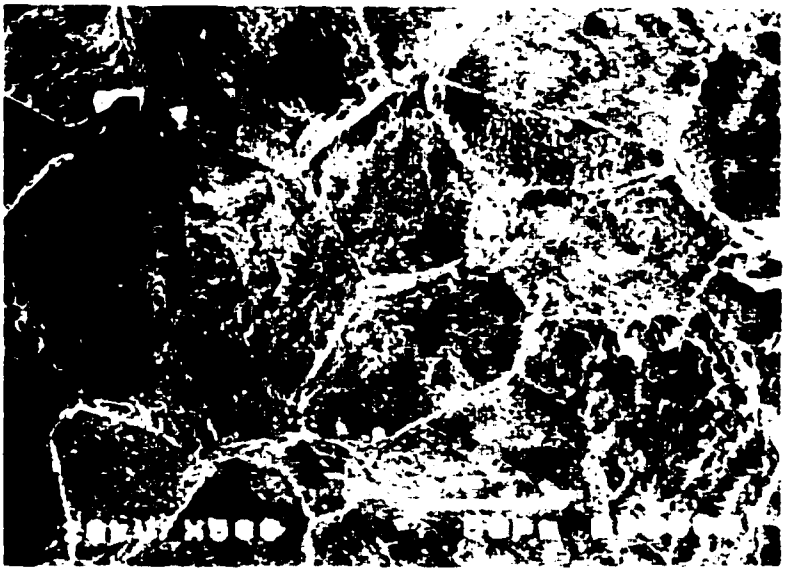

Figure 4.23. Brittle fracture with the solidification of weld metal grain boundaries clearly shown, 500X.

Figure 4.24. Another brittle fracture view of the same sample in figure 4.22, 500X.

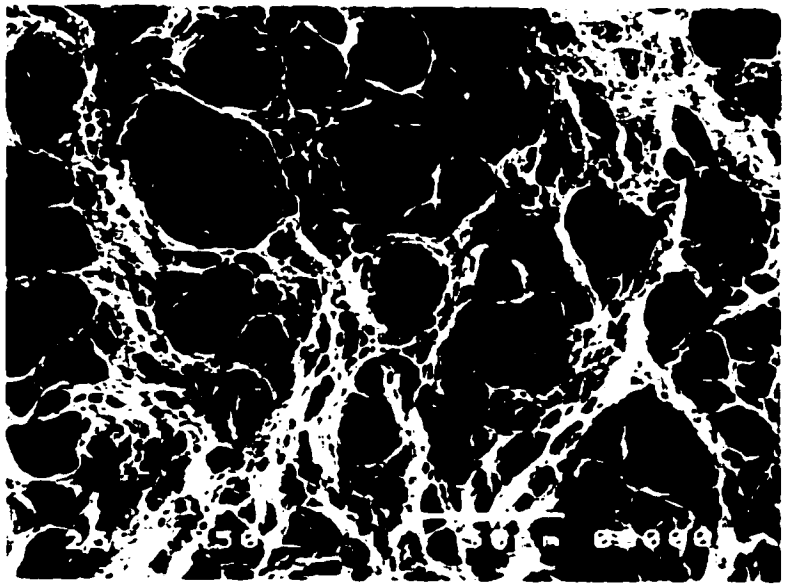

Figure (4.25). Micro void coalescence ductile fracture of the sample in figure 4.22, 500X.

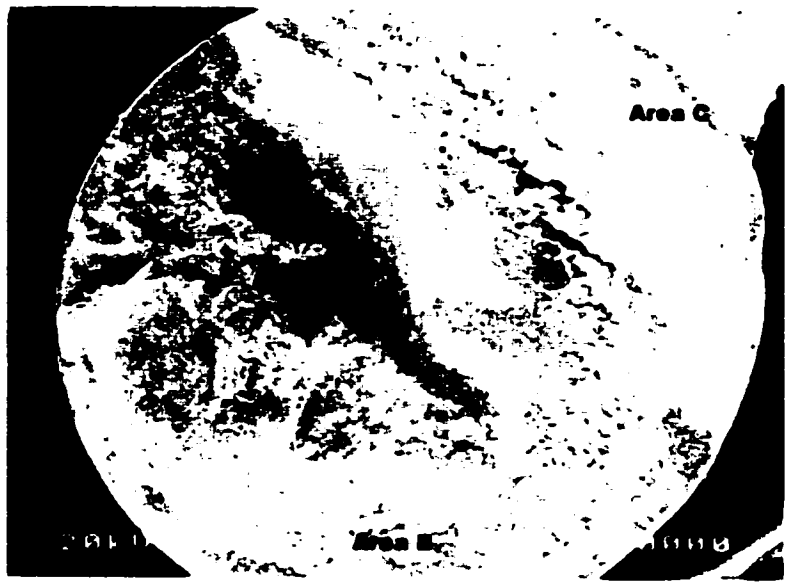

Figure 4.26. Low magnification SEM photograph of a fracture surface (s.s. aide) welded with Inco 182 @ 400°F preheat, 15X.

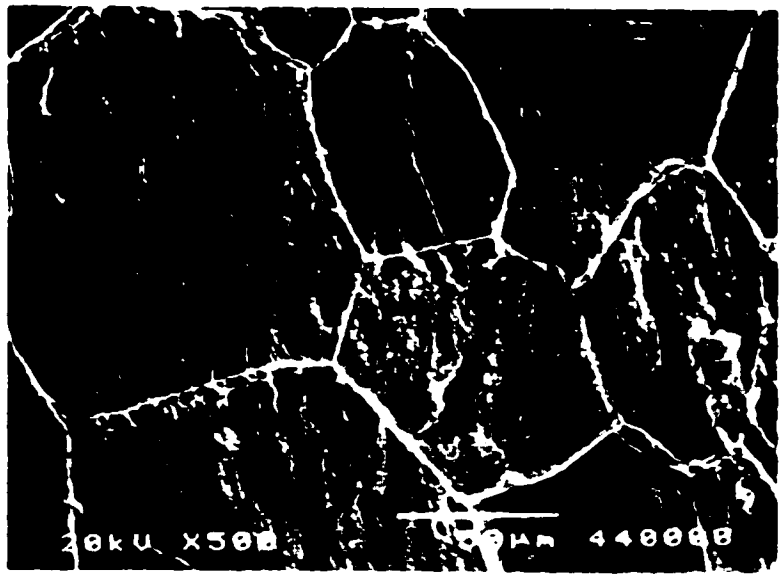

Figure 4.27. High magnification of area A from figure 4.26 for a brittle fracture region, 500X.

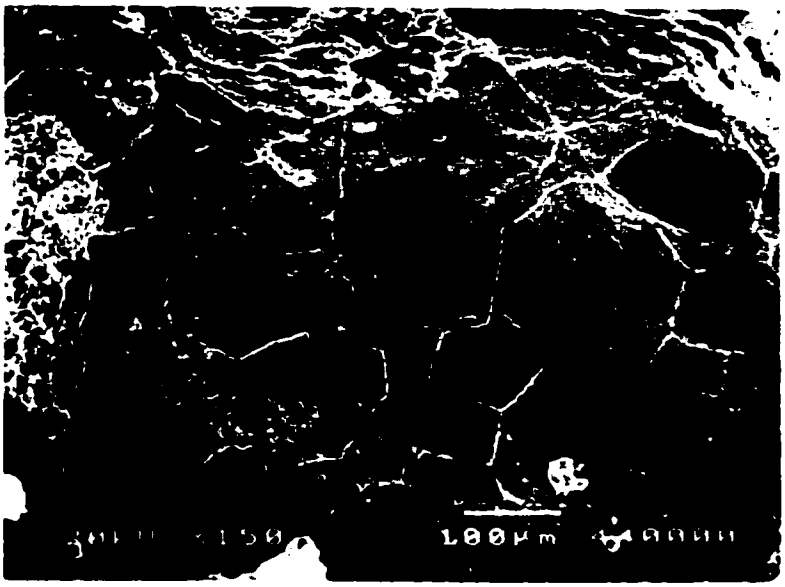

Figure 4.28. High magnification of area B from figure 4.26 for another brittle fracture region, 150X.

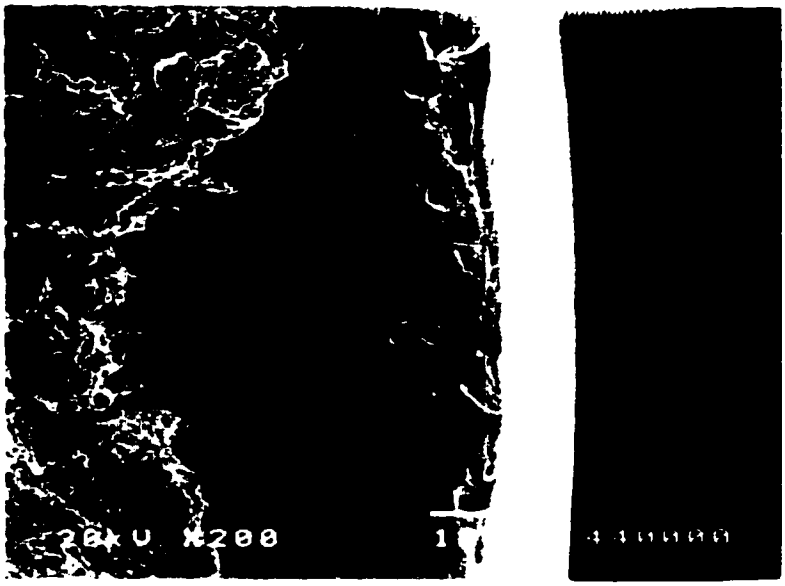

Figure 4.29. High magnification of area C from figure 4.26 for another brittle fracture region, 200X.

CHAPTER 5

CONCLUSION

The objective of this study is to assess the effect of sulfide stress cracking on the reliability of dissimilar metal weld specimens fabricated with different preheat temperatures and different welding electrodes (filler metals) exposed to a sour service environment.

Slight reduction in the yield strength was noticed as the welds preheating temperatures were increased, except at 400°F (205°C) for the Inco 182 welded samples, and at 350°F (177°C) for the E 309 welded samples. Similarly, slight decline in the ductility for both weld metals with increase in preheating temperature was noticed. This indicates that there was not much gain attained from the preheating process in term of reducing the yield strength or increasing the ductility. This could be due to the fact that preheating temperatures are not high enough to cause major, and significant microstructural alteration.

With reference to NACE standard TM 01-77-96 (which was used to determine the influence of SSC on DMWs), and based on the results presented on Time-To-Failure, it

can be said that both Inco 182 and E-309 electrodes produce welds with very high susceptibility to sulfide stress cracking. Nonetheless, there has been considerable improvement in the TTF for the Inco 182 welded samples at 400°F (205°C). This is in line with the findings in the literature reported by Omar [9-10], as the 400°F (205°C) is the optimum preheat temperature for the Inco 182 electrode in welding DMWs. On the other hand no consistent relation could be found between the preheating temperatures and the average time to failure for the E 309 welded samples.

An improvement in the TTF has been noticed as the %Y.S. loading decreases for both type of welded samples regardless the preheating temperature. Nontheless, most of the values for the estimated threshold stress value, which is the maximum stress the material can sustain without failure for 720 hrs or more, are below the standard design criteria used within Saudi Aramco (between 60 to 80 %Y.S.) and much below the acceptance criteria of 90% of the Y.S. published by the European Federation of Corrosion (90% of the Y. S).

Ranking of the preheat temperatures in terms of their postive effect on the TTF for the Inco 182 welded samples is as follows:

- The 400°F preheat temperature resulted in longest TTF at all leveles of applied stresses.
- At stress level between 35 and 55 ksi, 350°F and 450°F preheat result in the same time to failure.
- The 450°F preheat temperature was the 2nd best in term of its positive effect on TTF at all applied stress levels.
- And finally, the 350°F preheat temeprature was the worst in term of TTF.

Metallographic examination and Scanning Electron Microscope (SEM) characterization were used to assess the susceptibility and the failure modes. Energy Dispersive X-Ray Spectrometry (EDS) and Microhardness surveys were also performed to confirm the finding of previous analysis.

Visual examination of the samples after the NACE SSC test indicated that most of the failures were brittle failures along the weld fusion interface with the carbon steel base metal. Metallographic examination showed that cracks initiate at the hard zones and go along the fusion line between the carbon steel and the weld metal. The crack may propagate into the carbon steel HAZ. SEM examination of these samples indicated that two distinct fracture modes (Brittle and Ductile) were on all fractured surfaces.

Based on the results and findings obtained from the metallographical examination, and the EDS survey, it is apparent that filler metals with any appreciable chromium content will produce hard zone in the fusion line as presented. This explains why E 309 (Austenitic with 24 wt% Cr) was producing welds with very high amount of hard zone, and hence high susceptibility to SSC compare to Inco 182 (Ni-base with 15 wt %Cr).

Moreover, this study has indicated that the hard zones are still present even with the nickel-based electrodes, but that the size and frequency might be reduced, in comparison to the austenitic stainless steel electrodes. However, it does not appear that the hard zones can be reliably eliminated for manual welding methods, even with the nickel-base electrode, and the optimum preheat temperature.

In conclusion, Dissimilar Metal Welds fabricated in accordance to the stated welding conditions, and procedure are susceptible to sulfide stress cracking.

APPENDIX

EDS and microhardness surveys of some selected samples.

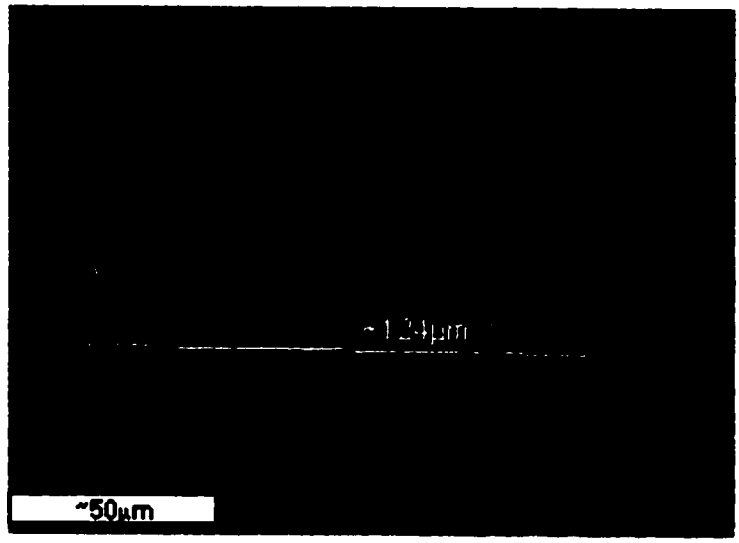

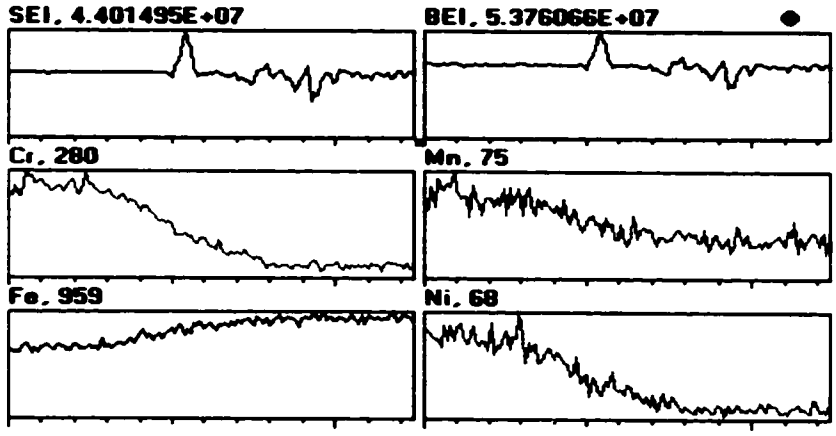

Microhardness identation (at three different positions) and EDS survey in the fusion line regoin for a sample welded with E 309 filler @ 400° F Preheat.

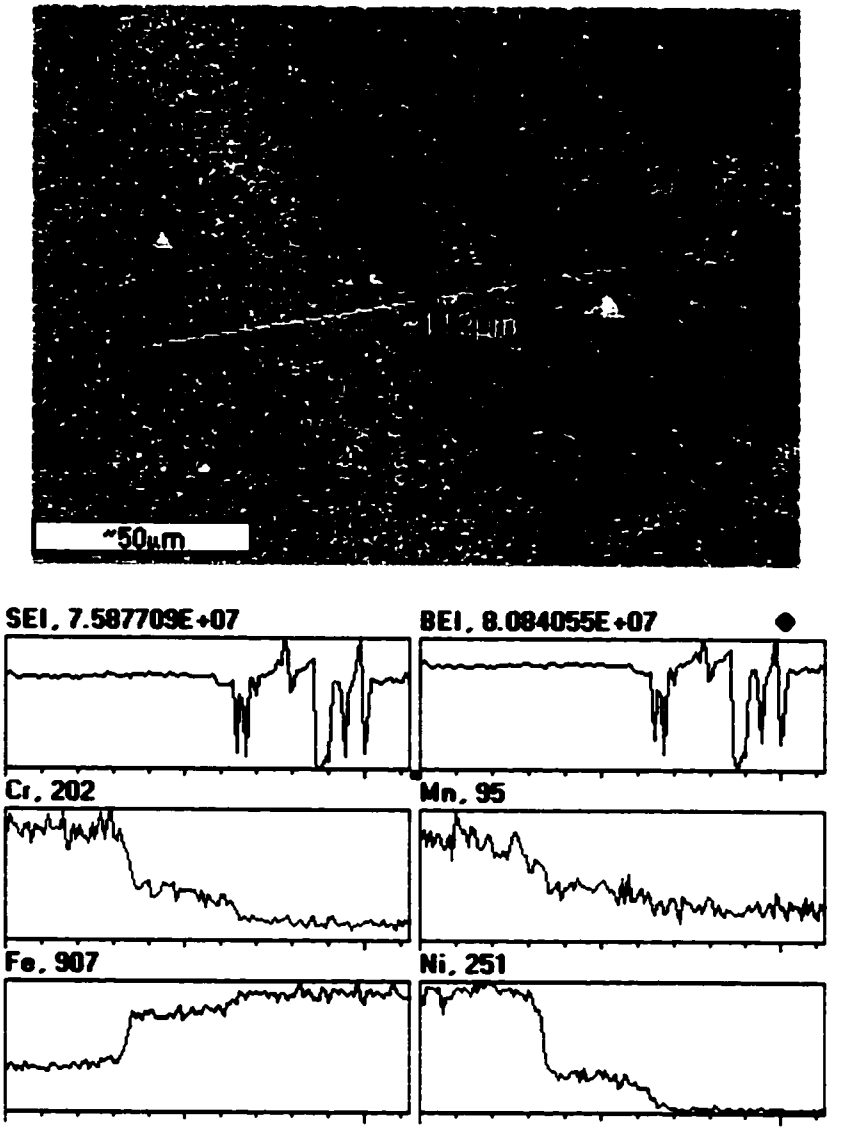

Microhardness identation (at three different positions) and EDS survey in the fusion line regoin for a sample welded with Inco 182 filler @ 400° F Preheat.

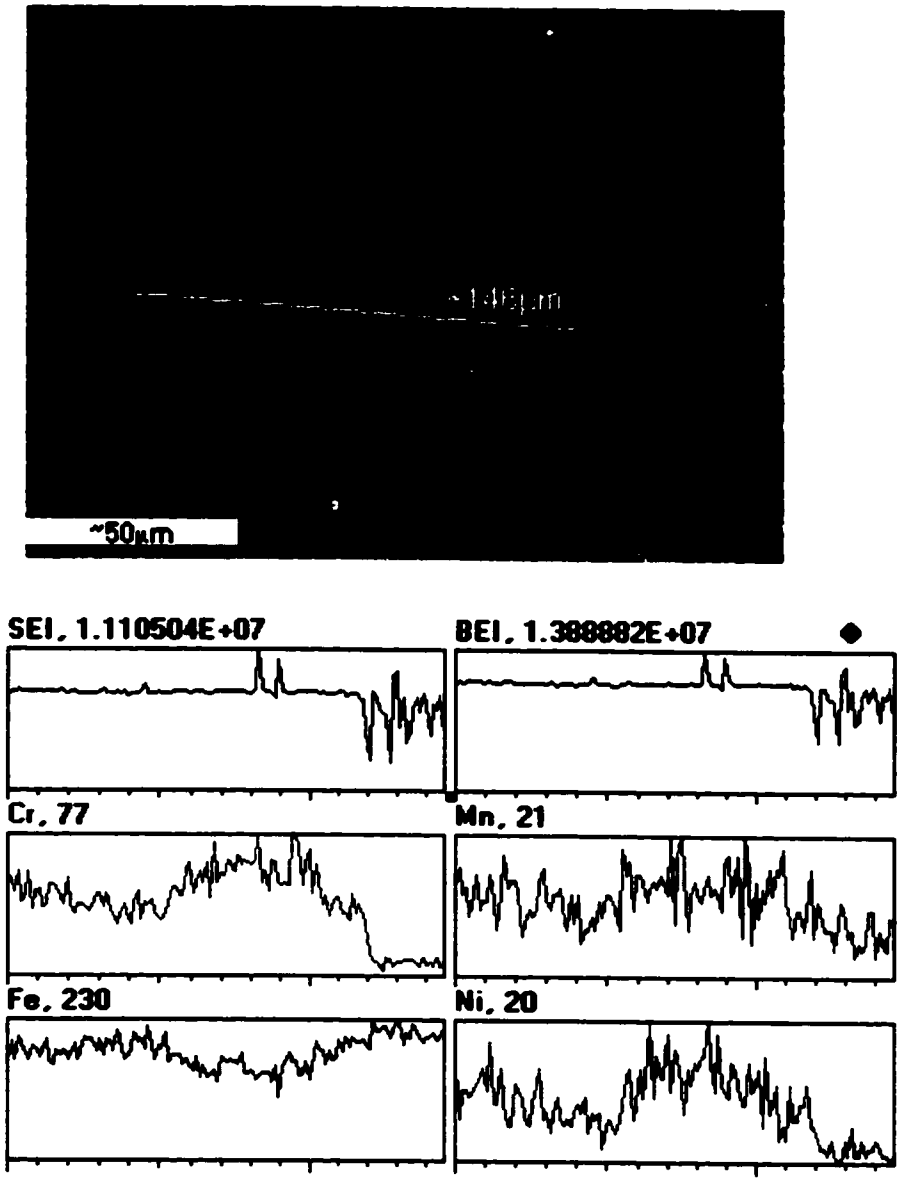

Microhardness identation (at three different positions) and EDS survey in the fusion line regoin for a sample welded with E 309 filler @ 350° F Preheat.

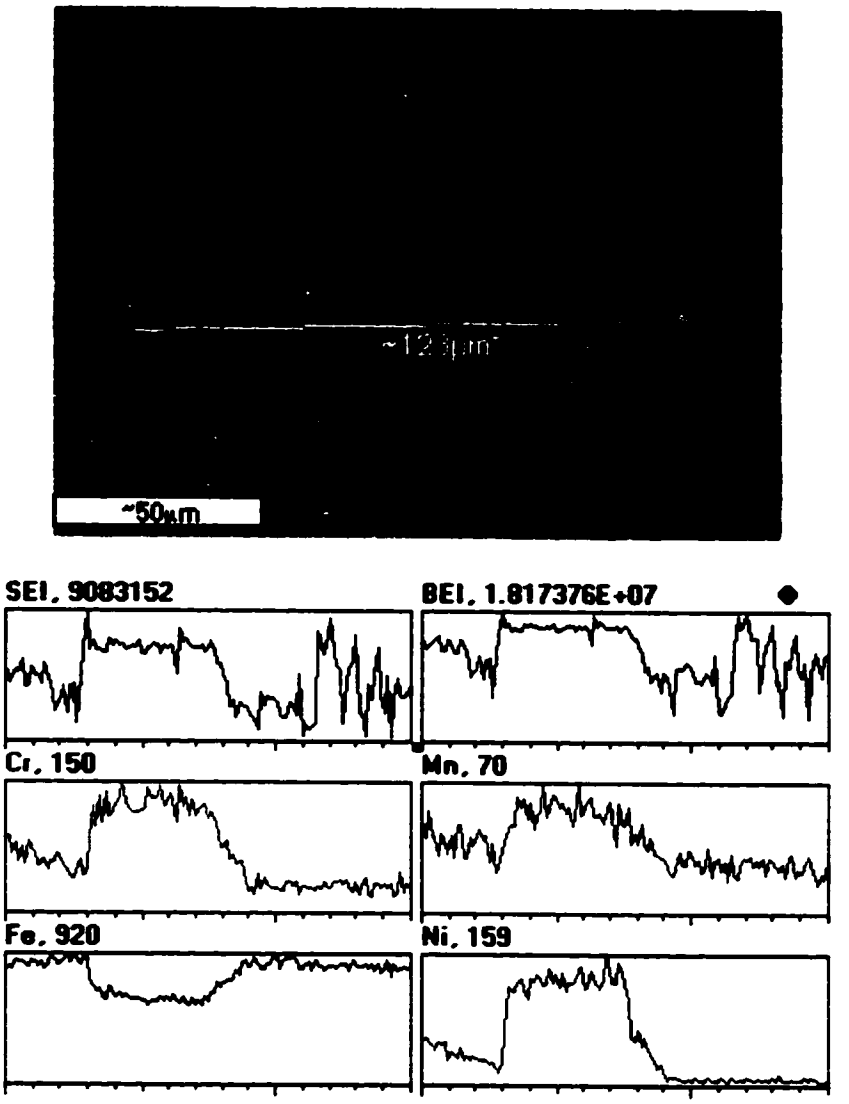

Microhardness identation (at three different positions) and EDS survey in the fusion line regoin for a sample welded with Inco 182 filler @ 450° F Preheat.

REFERENCES

1. Doody, T., "Intermediate Mixed Zones in Dissimilar Metal Welds for Sour Service". *Welding Journal*, March 1992, pp. 55 - 60.

2. NACE standard MR-01-75-95, "Sulfide Stress Cracking Resistant Metallic Materials for Oilfield Equipment", National Association of Corrosion Engineers (NACE), 1995.

3. ASM Handbook Vol. 11, Failure Analysis and Prevention, 9th edition, 1986.

4. Elboujdaini, M., Revie, R. W. Orr, R. F., Braid, J. E. M., and Lau, T. "Sulfide Stress Cracking Susceptibility of C/Mn & Cr/Mo Steels in Repair Welding". *NACE International Conference Proceedings*, Corrosion 94, paper number 72, 1994.

5. Corrosion in the Petrochemical Industry, Edited by Garverick, L. ASM, 1994.

6. Chan, S. L. I., Chien, L. W., and Chen, C. "Monitoring the Hydrogen Embrittlement of Dissimilar-Metal Weld in the Oil Industry". *Life Prediction of Corrodible Structure Conference Proceedings*, September 1991, pp. 65/1 - 65/11.

7. Schaefer, A. "Dissimilar Metal Weld Failure Problems in Large Steam Generators". *Power*, December 1979, pp. 68 - 69.

8. Lundin, C. D. "Dissimilar Metal Welds-Transition Joints Literature Review". *Welding Journal*, February 1982, pp. 58s - 63s.

9. Omar, A. A. "Welded Dissimilar Metals in Wet Sour Service", *5th Middle East Corrosion Conference Proceedings*, October 1991, pp. 453 - 468.

10. Omar, A. A. "Hard Zone at Dissimilar Metal Welds: Can we Prevent Their Formation". *Saudi Aramco Journal of Technology*, Winter 1996/97, pp. 51 - 57.

11. NACE Standard TM-01-77-96, "Laboratory Testing of Metals for Resistance to Sulfide Stress Cracking in H_2S Environments". National Association of Corrosion Engineers (NACE). 1996.

12. Craig, B. D., and Setterlund, R. B. "Catastrophic SSC Failure of a Dissimilar Metal Weld in a High Pressure Hydrogen Vessel". *NACE International Conference Proceedings*, Corrosion 91 Proceedings, March 1991, paper number 317.

13. "Sulfide Stress Cracking of Dissimilar Metal Welds". KFUPM/RI study report, PN# 25043, January 1991

14. Makhamreh, K. M., Aidun, and D. K. "Stress Corrosion Cracking of Flux Cored Iron Manganese Aluminum Weld Metal". *Welding Journal*, June 1993, pp 247s - 255s.

15. Onsqien, M. I., Aklselsen, O. M., Grong, Q., and Kvaale, P. E. "Prediction of Cracking Resistance in Steel Weldments". *Welding Journal*, January 1990, pp. 45 - 51.

16. Poeppeling, R. K., Pircher, H., and Sussek, G. "Influence of H_2S Concentration and Maximum Hardness of Welded Joints on the HSC Susceptibility of Low Alloy Steels". *NACE International Conference Proceedings*, Corrosion 94, paper no 75, 1994.

17. Van Wortel, J. C. "Integrity of Dissimilar Welded Joints in Hydrogen Service". *Stainless Steel World Journal*, Januray/February 2000, pp. 49 - 55.

18. Welding Metallurgy, by Linnert, G. E. 3rd edition, American Welding Society, New York, 1965.

19. Golovanenko, S. A., Zikeev, V. N., Serebyana, E. B., and Popova, L. V. "Effect of Alloying Elements and Structure on the Resistance of Structural Steels to Hydrogen Embrittlement". H_2S Corrosion in Oil and Gas Production- A compilation of Classic Papers, R. N. Tultle and R. D. Kane, Ed. NACE, 1982, pp. 198 - 204.

20. Irving, B. "Preheat : The Main Defense Against Hydrogen Cracking", Welding Journal, July 1992, pp. 25 -31.

21. "Guidelines on Materials Requirements for Carbon and Low Alloy Steels for H_2S Containing Environments in Oil and Gas Production". *European Federation of Corrosion Publication, Number 16*, The Institute of Metals 1995.